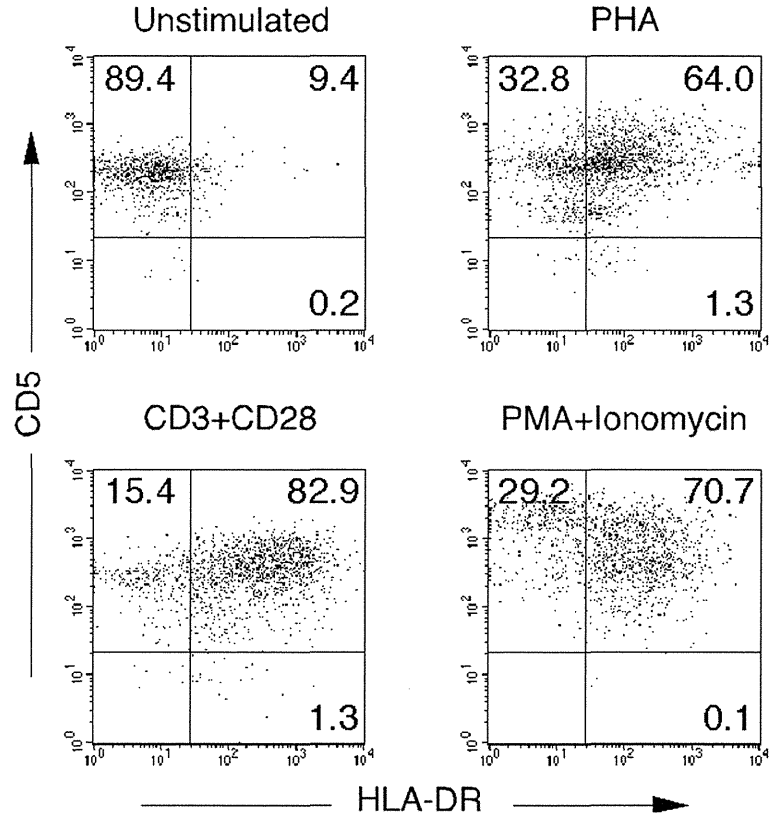

Fig. 3. Expression of CD5 after *in vitro* stimulation. PBMCs from normal controls were cultured for 72 h with phytohemagglutinin (PHA), with anti-CD3 (OKT3) plus anti-CD28 mAb, or with phorbol myristate acetate (PMA) plus ionomycin. Expression of CD5 and HLA-DR on $CD8^+$ T cells is shown.

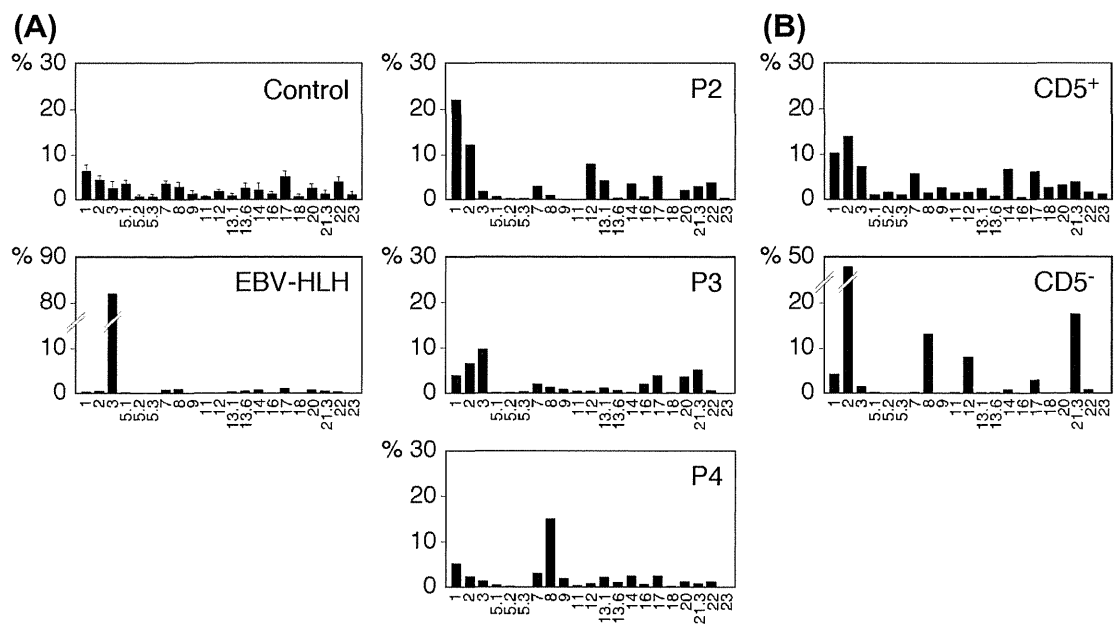

Fig. 4. TCR Vβ repertoire. (A) Peripheral blood samples were stained with monoclonal antibodies (mAbs) for individual TCR Vβ together with anti-CD4 and anti-CD8 mAbs. The percentage of TCR Vβ expression within the $CD8^+$ T cells was shown. (B) Peripheral blood samples were stained with mAbs for individual TCR Vβ subfamilies together with anti-CD8 and anti-CD5 mAbs. The percentage of TCR Vβ expression within the $CD5^+$ $CD8^+$ and $CD5^-$ $CD8^+$ T cells from patient P2 at 12 days of age was shown.

3.3. CD5 expression on normal T cells after in vitro stimulation

To assess whether down-regulation of CD5 was induced on normal T cells after simulation, PBMCs from three normal individuals were cultured for 72 h with phytohemagglutinin, anti-CD3 plus anti-CD28 mAbs, or phorbol myristate acetate plus ionomycin. Although normal $CD8^+$ T cells expressed activation marker HLA-DR after any of the stimulation, CD5 was not down-regulated (Fig. 3). We were not able to analyze expression of CD5 after *in vitro* stimulation using PBMCs from patients with FHL2 because

no appropriate samples were available, except for from patient P4. No down-regulation of CD5 was observed on the stimulated $CD8^+$ T cells from patient P4 (data not shown).

3.4. TCR Vβ repertoire of $CD8^+$ T cells

We have previously demonstrated that activated and EBV-infected $CD8^+$ T cells with down-regulation of CD5 proliferated clonally in patients with EBV–HLH [5]. To assess clonality of the $CD8^+$ T cells from patients with FHL2, we investigated the diversity of the TCR Vβ repertoire in $CD8^+$ T cells by flow cytometry (Fig. 4A). Although a massive expansion of a specific TCR Vβ has often been demonstrated for $CD8^+$ T cells from patients with EBV–HLH, $CD8^+$ T cells from patients with FHL2 exhibited oligoclonal or polyclonal proliferation. Oligoclonal expansion was more prominent in $CD5^-$ $CD8^+$ T cells than in $CD5^+$ $CD8^+$ T cells from patient P2 at 12 days of age (Fig. 4B).

4. Discussion

HLH is a heterogeneous group of diseases that are characterized by uncontrolled proliferation of activated macrophages and T cells with overproduction of pro-inflammatory cytokines [1,2]. Activated $CD8^+$ T cells are frequently observed during the acute phase of HLH. We have recently described the clinical significance of down-regulation of CD5 on activated and clonally-expanded $CD8^+$ T cells that were predominantly infected by EBV in patients with EBV–HLH [5]. However, down-regulation of CD5 is likely a general consequence of the dysregulated proliferation of $CD8^+$ T cells. Increased subpopulations of $CD5^-$ $CD8^+$ T cells have been reported in patients with allogeneic bone marrow transplantation, human immunodeficiency virus-1 infection, acute herpes virus infections and peripheral T-cell neoplasma [19–22]. In addition, a 17-day-old patient with FHL2 has been reported to exhibit uncontrolled proliferation of $CD5^-$ $CD8^+$ T cells that showed massive infiltration into the liver [11]. We therefore investigated whether this unusual subset of $CD5^-$ $CD8^+$ T cells was generally present in FHL2, which represents most common form of FHL.

In the present study, we demonstrated a significant increase in the subpopulation of $CD5^-$ $CD8^+$ T cells in all patients with FHL2, compared with control participants. These cells expressed HLA-DR antigen, indicating an activated phenotype. In contrast to EBV–HLH in which expanded $CD8^+$ T cells often reacted with a specific TCR Vβ mAb reflecting clonal proliferation of EBV-infected cells [5], $CD8^+$ T cells from patients with FHL2 exhibited much milder restriction in TCR Vβ repertoire suggesting reactive proliferation. This unique subset of $CD5^-$ HLA-DR^+ $CD8^+$ T cells in FHL2 was detectable only in the acute phase of HLH in which patients exhibited hypercytokinemia, and declined progressively after successful treatment concomitant with the levels of serum ferritin, soluble IL-2 receptor and pro-inflammatory cytokines. Thus, serial analysis of CD5 expression and activation markers on $CD8^+$ T cells may represent an additional valuable tool for the follow-up of patients with FHL2. Moreover, this profile might provide us with clinical clues to suspect FHL2 during the initial flow cytometric assessment of lymphocyte subsets with a small amount of peripheral blood.

The mechanism underlying down-regulation of CD5 on activated $CD8^+$ T cells from patients with FHL2, as well as with EBV–HLH, remains to be elucidated. It is also unknown whether $CD8^+$ T cells from other HLH cases exhibit similar profiles during the acute phase. Failure of the down-regulation of CD5 on normal $CD8^+$ T cells after *in vitro* stimulation suggests that this profile indicates the highly dysregulated activation and proliferation of $CD8^+$ T cells *in vivo* in the setting of HLH. On the other hand, studies of T cells from CD5-deficient mice have reported hyperresponsiveness of $CD5^-$ T cells to TCR stimulation, suggesting that down-regulation of CD5 might contribute to the uncontrolled proliferation of $CD8^+$ T cells in FHL2. Further studies are necessary to address these issues. Because a variety of primary and secondary causes of HLH lead to similar clinical and biological features, and HLH can range from a self-limited episode to a rapidly fatal course [11], it is necessary to identify a parameter that can predict severe cases of HLH, for which the timely initiation of life-saving therapy would be required. Further investigations are underway to determine whether down-regulation of CD5 on activated $CD8^+$ T cells could distinguish severe cases of HLH from other inflammatory conditions, including mild cases of HLH.

In summary, our studies demonstrate the increased subpopulation of activated $CD8^+$ T cells with down-regulation of CD5 in the acute phase of FHL2, and point to an additional aspect of the immune dysregulation in this disease.

Acknowledgments

We thank Dr. Hirokazu Kanegane for help with sequence analysis, and Ms. Harumi Matsukawa and Ms. Shizu Kouraba for their excellent technical assistance. This work was supported by a Grant-in-Aid for Scientific Research from the Ministry of Education, Culture, Sports, Science and Technology of Japan; and a Grant from the Ministry of Health, Labour, and Welfare of Japan, Tokyo.

References

[1] Jordan MB, Allen CE, Weitzman S, Filipovich AH, McClain KL. How I treat hemophagocytic lymphohistiocytosis. Blood 2011;118:4041.
[2] Usmani GN, Woda BA, Newburger PE. Advances in understanding the pathogenesis of HLH. Br J Haematol 2013.
[3] Nagai K, Yamamoto K, Fujiwara H, An J, Ochi T, Suemori K, et al. Subtypes of familial hemophagocytic lymphohistiocytosis in Japan based on genetic and functional analyses of cytotoxic T lymphocytes. PLoS One 2010;5:e14173.
[4] Ishii E, Ohga S, Imashuku S, Yasukawa M, Tsuda H, Miura I, et al. Nationwide survey of hemophagocytic lymphohistiocytosis in Japan. Int J Hematol 2007;86:58.
[5] Toga A, Wada T, Sakakibara Y, Mase S, Araki R, Tone Y, et al. Clinical significance of cloned expansion and CD5 down-regulation in Epstein-Barr virus (EBV)-infected $CD8^+$ T lymphocytes in EBV-associated hemophagocytic lymphohistiocytosis. J Infect Dis 2010;201:1923.
[6] Bierer BE, Nishimura Y, Burakoff SJ, Smith BR. Phenotypic and functional characterization of human cytolytic T cells lacking expression of CD5. J Clin Invest 1988;81:1390.
[7] Lozano F, Simarro M, Calvo J, Vila JM, Padilla O, Bowen MA, et al. CD5 signal transduction: positive or negative modulation of antigen receptor signaling. Crit Rev Immunol 2000;20:347.
[8] Friedlein G, El Hage F, Vergnon I, Richon C, Saulnier P, Lecluse Y, et al. Human CD5 protects circulating tumor antigen-specific CTL from tumor-mediated activation-induced cell death. J Immunol 2007;178:6821.
[9] Dalloul A. CD5: a safeguard against autoimmunity and a shield for cancer cells. Autoimmun Rev 2009;8:349.
[10] Brossard C, Semichon M, Trautmann A, Bismuth G. CD5 inhibits signaling at the immunological synapse without impairing its formation. J Immunol 2003;170:4623.
[11] Karandikar NJ, Kroft SH, Yegappan S, Rogers BB, Aquino VM, Lee KM, et al. Unusual immunophenotype of $CD8^+$ T cells in familial hemophagocytic lymphohistiocytosis. Blood 2004;104:2007.
[12] Henter JI, Horne A, Arico M, Egeler RM, Filipovich AH, Imashuku S, et al. HLH-2004: diagnostic and therapeutic guidelines for hemophagocytic lymphohistiocytosis. Pediatr Blood Cancer 2007;48:124.
[13] Nishi M, Nishimura R, Suzuki N, Sawada A, Okamura T, Fujita N, et al. Reduced-intensity conditioning in unrelated donor cord blood transplantation for familial hemophagocytic lymphohistiocytosis. Am J Hematol 2012;87:637.
[14] Wada T, Muraoka M, Yokoyama T, Toma T, Kanegane H, Yachie A. Cytokine profiles in children with primary Epstein-Barr virus infection. Pediatr Blood Cancer 2013;60:E46.
[15] Okajima M, Wada T, Nishida M, Yokoyama T, Nakayama Y, Hashida Y, et al. Analysis of T cell receptor Vβ diversity in peripheral $CD4^+$ and $CD8^+$ T lymphocytes in patients with autoimmune thyroid diseases. Clin Exp Immunol 2009;155:166.
[16] Keerthikumar S, Raju R, Kandasamy K, Hijikata A, Ramabadran S, Balakrishnan L, et al. RAPID: resource of asian primary immunodeficiency diseases. Nucleic Acids Res 2009;37:D863.

[17] Wada T, Seki H, Konno A, Ohta K, Nunogami K, Kaneda H, et al. Developmental changes and functional properties of human memory T cell subpopulations defined by CD60 expression. Cell Immunol 1998;187:117.
[18] Hijikata, A.; Raju, R.; Keerthikumar, S.; Ramabadran, S.; Balakrishnan, L.; Ramadoss S.K.; *et al.*, Mutation@a glance: an integrative web application for analysing mutations from human genetic diseases. DNA research: an International journal for rapid publication of reports on genes and genomes **17** (2010) 197.
[19] Bierer BE, Burakoff SJ, Smith BR. A large proportion of T lymphocytes lack CD5 expression after bone marrow transplantation. Blood 1989;73:1359.
[20] Indraccolo S, Mion M, Zamarchi R, Coppola V, Calderazzo F, Amadori A, et al. A $CD3^+$ $CD8^+$ T cell population lacking CD5 antigen expression is expanded in peripheral blood of human immunodeficiency virus-infected patients. Clin Immunol Immunopathol 1995;77:253.
[21] Borthwick NJ, Bofill M, Hassan I, Panayiotidis P, Janossy G, Salmon M, et al. Factors that influence activated $CD8^+$ T-cell apoptosis in patients with acute herpesvirus infections: loss of costimulatory molecules CD28, CD5 and CD6 but relative maintenance of Bax and Bcl-X expression. Immunology 1996;88:508.
[22] Jamal S, Picker LJ, Aquino DB, McKenna RW, Dawson DB, Kroft SH. Immunophenotypic analysis of peripheral T-cell neoplasms. A multiparameter flow cytometric approach. Am J Clin Pathol 2001;116:512.

Speaking the same language: The World Allergy Organization Subcutaneous Immunotherapy Systemic Reaction Grading System. J Allergy Clin Immunol. 2010;125(3):569-74, 574 e561-74 e567.
5. Paniagua MJ, Bosque M, Asensio O, Larramona H, Marco MT. Immunotherapy with acarus extract in children under the age of 5 years. Allergol Immunopathol. 2002;30(1):20-4.
6. Schubert R, Eickmeier O, Garn H, Baer PC, Mueller T, Schulze J, Rose MA, Rosewich M, Renz H, Zielen S.. Safety and immunogenicity of a cluster specific immunotherapy in children with bronchial asthma and mite allergy. Int Arch Allergy Immunol. 2009;148(3):251-60.
7. Garde J, Ferrer A, Jover V, Pagan JA, Andreu C, Abellan A, Félix R, Milán JM, Pajarón M, Huertas AJ, Lavín JR, de la Torre F. Tolerance of a Salsola kali extract standardized in biological units administered by subcutaneous route. Multicenter study. Allergol Immunopathol. 2005;33(2):100-4.
8. Guardia P, Moreno C, Justicia JL, Conde J, Cimarra M, Díaz M, Guerra F, Martínez-Cócera C, Gonzalo-Garijo MA, Pérez-Calderón R, González-Quevedo T, Sánchez-Cano M, Vigaray J, Acero S, Blanco R, Martín S, de la Torre F.. Tolerance and short-term effect of a cluster schedule with pollen-extracts quantified in mass-units. Allergol Immunopathol. 2004;32(5):271-7.
9. García-Catalán M, Cruz M, Bosque M, Larramona H, Asensio O, Grau R. Safety of a cluster-immunotherapy with a depot allergoid in pediatric patients. Allergy. 2008. 63(88):158-611. A649.
10. Cox L. Accelerated immunotherapy schedules: review of efficacy and safety. Ann Allergy Asthma Immunol. 2006;97(2):126-137; quiz 137-140, 202.

Manuscript received June 8, 2012; accepted for publication, August 23, 2012.

Montserrat Bosque
Pediatric Allergology and Pneumology Unit
Hospital de Sabadell – Fundació Universitària
Parc Taulí Universitat Autònoma de Barcelona
Parc Taulí 1, 08208 Sabadell, Barcelona, Spain
E-mail: mbosque@tauli.cat

Novel Mutation of *IL2RG* Gene in a Korean Boy With X-linked Severe Combined Immunodeficiency

YW Lee,[1] EA Yang,[1] HJ Kang,[2] X Yang,[3] N Mitsuiki,[4,5] O Ohara,[4,6] T Miyawaki,[3] H Kanegane,[3] JH Lee[1]
[1]*Department of Pediatrics, Chungnam National University School of Medicine, Daejeon, Korea*
[2]*Department of Pediatrics, Cancer Research Institute, Seoul National University College of Medicine, Seoul, Korea*
[3]*Department of Pediatrics, Graduate School of Medicine and Pharmaceutical Sciences, University of Toyama, Toyama, Japan*
[4]*Department of Human Genome Research, Kazusa DNA Research Institute, Kisarazu, Chiba, Japan*
[5]*Division of Pediatrics and Developmental Biology, Tokyo Medical and Dental University Graduate School, Tokyo, Japan*
[6]*Laboratory for Immunogenomics, Research Center for Allergy and Immunology, RIKEN Yokohama Institute, Yokohama, Japan*

Key words: XSCID. IL-2 receptor. Mutation. Wheezing.

Palabras clave: XSCID. Receptor IL-2. Mutación. Sibilancias.

Severe combined immunodeficiency (SCID) represents a group of rare, sometimes fatal, genetic disorders in which the adaptive immune system is impaired. X-linked SCID (X-SCID) occurs in approximately 50% of patients with SCID and is immunologically characterized by markedly diminished numbers of T cells and natural killer (NK) cells and normal or slightly increased numbers of dysfunctional B cells ($T^-B^+NK^-$ SCID) [1]. Affected patients have a profound deficiency of both cellular and humoral immunities [2,3]. X-SCID is mapped to the Xq13.1 locus and is caused by mutations in the *IL2RG* gene encoding the interleukin 2 receptor (IL-2R) γ chain (common γ chain), which is also associated with cytokine receptors for IL-4, IL-7, IL-9, IL-15, and IL-21 [4]. Therefore, cytokine signaling through the common γ chain is impaired in patients with X-SCID, leading to the impaired development of T and NK cells [4]. Various types of mutation in the *IL2RG* gene have been described in patients with X-SCID. We describe the case of a 5-month-old Korean male with X-SCID who had a novel mutation in the *IL2RG* gene.

A 5-month-old male infant with recurrent bronchiolitis was referred to Chungnan National University Hospital. His weight was 6.3kg (fifth percentile) and his height was 63.9 cm (25th percentile). The patient was born at 39 weeks of gestation after a normal pregnancy and delivery; however, his birth weight was 2.2 kg and there had been intrauterine growth retardation. There was no history of consanguinity in the family. His family history disclosed that 2 maternal uncles had died of infection during the first year of life. From the age of 3 months, the patient had frequently visited and had been admitted to a primary hospital because of recurrent bronchiolitis.

Physical examination on admission showed an emaciated infant with an otherwise normal appearance. The patient had undergone regular scheduled vaccinations until the age of 2 months (BCG, diphtheria-tetanus-acellular pertussis, polio-first shot, hepatitis B virus-second shot), but had not been vaccinated thereafter. He had a BCG scar, but no lymphadenopathy, organomegaly, or skin rash. Rales and expiratory wheezing were positive on auscultation. Human respiratory syncytial virus A antigen was detected in the tracheal aspirated fluid. Computed tomography of the chest revealed bronchial wall thickening with no apparent thymus. The blood counts on admission included white blood cells of 6630/μL (49.3% neutrophils and 35.6% lymphocytes), hemoglobin of 13.1 g/dL, and platelets of 384 000/μL. The patient had absolute lymphopenia (2360/uL). Further investigation demonstrated hypogammaglobulinemia (immunoglobulin [Ig] G, 109mg/dL; IgM,10 mg/dL; IgA, 1mg/dL, and IgE, 0.1 IU/mL) with marked reduction of T cells and NK cells and an increased percentage of B cells (94.3%). Proliferative responses of peripheral blood cells to mitogens were markedly decreased. These results implied $T^-B^+NK^-$SCID. On the basis of the family history, recurrent infections, absence of thymus, failure to thrive, and deficiency of cellular and humoral immunity, X-SCID was suspected.

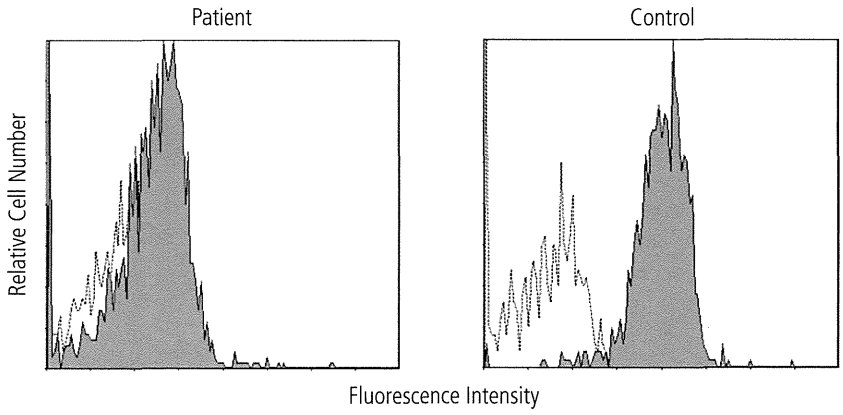

Figure. Interleukin 2 receptor γ (CD132) expression in $CD20^+$ B cells from the patient and a healthy control. Cells were incubated with phycoerythrin-conjugated anti-CD132 monoclonal antibody (clone: TUGh4) and fluorescein isothiocyanate-conjugated anti-CD20 monoclonal antibody, and were analyzed using a flow cytometer. The dotted lines represent the negative control stained with isotype control antibody. The filled areas represent CD132-specific staining.

Blood samples were obtained from the patient and his mother following informed consent. Flow cytometry demonstrated deficient expression of the IL-2R γ chain (CD132) on $CD20^+$ B cells in the patient, indicating IL-2R γ chain deficiency or X-SCID (Figure). The 8 exons and surrounding genomic sequences of the *IL2RG* gene were amplified from genomic DNA as previously described and directly sequenced [5]. A single base insertion at exon 6 (854insG), which resulted in a frameshift mutation (Thr286AspfsX1), was detected in the patient. His clinical course was complicated by recurrent regurgitation, diarrhea, acute suppurative otitis media, and persistent bronchiolitis. At the age of 8 months, he underwent cord blood stem cell transplantation without conditioning at Seoul National University Hospital. The posttransplant course was complicated by grade 1 graft versus host disease of the skin, and the disease responded to prednisolone. However, the patient died of treatment-related complications 1 month after transplantation.

We identified a novel mutation of the *IL2RG* gene in a Korean infant with X-SCID. The patient showed classical clinical features and laboratory data, such as absolute lymphopenia, low percentages of T cells and NK cells, and an increased number of B cells. He was found to have a single nucleotide (guanine) insertion at position 854+1 (854insG) within exon 6, resulting in a frameshift amino acid change. No mutations have been identified at position 854 in the *IL2RG* gene, although many different mutations involving other nucleotide positions in exon 6 have been confirmed. This may be the second genetically identified case of X-SCID in Korea. The first patient showed a single point mutation (C690T) with a missense mutation (R226C), which has been previously reported in many ethnic backgrounds[6]. A total of 344 mutation entries, comprising 198 unique molecular events, are now present in the X-linked SCID mutation database (IL2RGbase) (http://research.nhgri.nih.gov/scid/). Many types of mutation have been reported throughout all 8 exons of the *IL2RG* gene.

In conclusion, we have reported a novel mutation of the *IL2RG* gene in a patient with X-SCID. A diagnosis of SCID should be suspected in patients with persistent infection and absolute lymphopenia in early infancy, as occurred in our patient. We believe we might have reported the second case of X-SCID and the third case of SCID including IL-7Rα chain deficiency in Korea [7]. There may be more Korean patients with SCID. Further studies of X-SCID in this country are needed to clarify the differences observed in mutations and disease between different ethnic groups. Neonatal screening of the measurement of the T cell receptor excision circle is useful for detecting patients with SCID and severe T lymphopenia[8]. This method has been applied in some states in the United States, and it may be applicable in Korea.

Acknowledgments

This study was partly supported by the Basic Science Research Program through the National Research Foundation of Korea (NRF) funded by the Ministry of Education, Science and Technology (2011-0021633) and Grants-in-Aid for Scientific Research from the Ministry of Education, Culture, Sports and Technology and grants from the Ministry of Health, Labor and Welfare of Japan. We thank Ms Chikako Sakai and Mr Hitoshi Moriuchi for their technical assistance.

References

1. Buckley RH, Schiff RI, Schiff SE, Markert ML, Williams LW, Harville TO, Roberts JL, Puck JM. Human severe combined immunodeficiency (SCID): generic, phenotypic and functional diversity in 108 infants. J Pediatr. 1997;130:378-87.
2. Fischer A. Severe combined immunodeficiencies (SCID). Clin Exp Immunol. 2000;122:143-49.
3. Al-Herz W, Bousfiha A, Casanova JL, Chapel H, Conley ME, Cunningham-Rundles C, Etzioni A, Fischer A, Franco JL, Geha RS, Hammarström L, Nonoyama S, Notarangelo LD, Ochs HD, Puck JM, Roifman CM, Seger R, Tang MLK. Primary immunodeficiency diseases: an update on the classification from the international union of immunological societies expert committee for primary immunodeficiency. Front Immunol. 2011;2:54.
4. Sugamura K, Asao H, Kondo M, Tanaka N, Ishii N, Ohbo K, Nakamura M, Takeshita T. The interleukin-2 receptor γ-chain: its role in the multiple cytokine receptor complexes and T cell development in XSCID. Annu Rev Immunol. 1996;14:179-205.
5. Kumaki S, Ochs HD, Timour M, Schooley K, Ahdieh M, Hill H, Sugamura K, Anderson D, Zhu Q, Cosman D, Giri JG. Characterization of B cell lines established from two X-linked severe combined immunodeficiency patients: interleukin-15 binds to the B cells but is not internalized efficiently. Blood. 1995;86:1428-36.
6. Jo EK, Kumaki S, Wei D, Tsuchiya S, Kanegane H, Song CH, Noh HY, Kim YO, Kim SY, Chung HY, Kim YH, Kook H. X-linked severe combined immunodeficiency syndrome: the first Korean case with γc chain gene mutation and subsequent genetic counseling. J Korean Med Sci. 2004;19:123-6.
7. Jo EK, Kook H, Uchiyama T, Hakozaki I, Kim YO, Song CH, Park JK, Kanegane H, Tsuchiya Shigeru, Kumaki S. Characterization of a novel nonsense mutation in the interleukin-7 receptor α gene in a Korean patient with severe combined immunodeficiency. Int J Hematol. 2004;80:332-5.
8. Chase NM, Verbsky JW, Routes JM. Newborn screening for SCID: three years of experience. Ann N Y Acad Sci. 2011;1238:99-105.

Manuscript received June 26, 2012; accepted for publication, August 30, 2012.

Jae Ho Lee
Department of Pediatrics
Chungnam National University School of Medicine
282 Munhwa-ro, Jung-gu
Daejeon 301-721, Korea
E-mail: immlee@cnu.ac.kr

Food Allergy to Caper (*Capparis spinosa*)

M Alcántara,[1] M Morales,[2] J Carnés[2]
[1]*Allergy Department, Complejo Hospitalario de Jaén, Jaén, Spain*
[2]*R&D Department, Laboratorios LETI, Tres Cantos, Madrid, Spain*

Key words: *Capparis spinosa*. Caper. Food allergy. Mustard. Pro-hevein. Hev b 6.

Palabras clave: *Capparis spinosa*. Alcaparra. Alergia a alimentos. Mostaza. Pro-heveina. Hev b 6.

Capparis spinosa is a bush that belongs to the Capparaceae family, member of the Brassicales order, as well as the mustard family (Brassicaceae), whose ability to induce allergic symptoms has been well documented, with several allergens described [1,2]. *C spinosa* is typical of the Mediterranean region. Its buds and fruits are eaten pickled, as a snack, seasoning, or as part of sauces. Moreover, members of the Capparaceae family have numerous medical applications thanks to their antimicrobial, antioxidative, anti-inflammatory, immunomodulatory, and antiviral properties [3-5]. All the species of this family contain *iso*thiocyanate (mustard oil), and are therefore expected to irritate the skin [6]. There have been reports of contact dermatitis due to *C spinosa* [7], but to the best of our knowledge, the present study is the first to report allergy following the ingestion of caper fruit.

We describe a 24-year-old man who reported allergic symptoms after the ingestion of shellfish paella and caper fruit. He presented at the emergency department of Complejo Hospitalario in Jaén, Spain, with redness, angioedema of the face and hands, and aphonia. The patient was treated with methylprednisolone and dexchlorpheniramine. After several hours under observation, he was discharged with antihistamine and oral corticosteroid treatment.

The patient had previously been diagnosed as allergic to *Olea europaea* and grasses, and experienced rhinoconjunctivitis and moderate, persistent asthma in the spring. However, he had not previously presented allergic reactions to food.

The patient was skin-prick tested with a battery of standardized aeroallergens including grasses, *Salsola kali, Chenopodium album, Cupressus arizonica, Parietaria judaica, Ambrosia elatior, O europaea*, and *Platanus hybrida*, mites (*Dermatophagoides*), epithelia (cat and dog), mold (*Alternaria alternata*), *Anisakis simplex*, and latex (Bial-Aristegui). The results were positive for *Lolium perenne* (wheal diameter, 8 mm), *Cynodon dactylon* (4 mm), and *O europaea* (9 mm), and negative in all other cases. We also performed prick to prick tests with mustard, clam, shrimp, squid, caper bud, and caper fruit.

In the United States the regulation of nonstandardized AEs presented some similarities with our approach. AEs were classified into 4 categories according to scientific data supporting their use in diagnosis and treatment, and the extracts were regularly evaluated by the regulatory agencies. The last update was conducted between 2003 and 2011, and the process was recently reviewed by Slater et al.[1] It was shown that for nearly half of nonstandardized AEs there were, in fact, little or no data to support their effectiveness. We had similar results: 66 of 84 AEs were validated for diagnosis, but only for 29 of 66 was there at least 1 published piece of data to support their effectiveness for immunotherapy (Table I). Among those 66 authorized AEs, approximately one third are standardized. There is no consensus about the standardization methods, and the European approaches present some differences compared with the US approach (see Table E1 in this article's Online Repository at www.jacionline.org). Briefly, in-house reference preparation (IHRP) AEs are standardized *in vivo* and *in vitro*. Each manufacturer has its own IHRP, and there is no national standard. Batch-to-batch standardization is performed *in vitro* through a comparison of the AEs with the IHRP.[9]

In the future, the NPP list will be updated every 5 years, and requests for MA will be made and processed for standardized AEs produced industrially and frequently used for immunotherapy.

In conclusion, for the first time in Europe, this work guarantees that available AEs are clinically relevant and safe. Moreover, it guarantees that all AEs comply with recent European guidelines on APs, including rare allergens for which it is not possible to obtain large clinical studies requested for MA. The process involved all the representatives of allergists and manufacturers and is still ongoing.

Frédéric de Blay, MD[a,b]
Virginie Doyen, MD[b,c]
Evelyne Bloch-Morot, MD[d]
Daniel Caillot, MD[e]
Jacques Gayraud, MD[f]
Aymar de Laval, MD[e]
Alain Thillay, MD[g]
*for the APSI group**

From [a]the French Society of Allergology (SFA), Paris, France; [b]the Division of Allergy, Department of Respiratory Disease, University Hospital of Strasbourg and University of Strasbourg, Strasbourg, France; [c]the Clinic of Immuno-Allergology, CHU Brugmann, Université Libre de Bruxelles (ULB), Brussels, Belgium; [d]the French Association for Continual Medical Education of Allergists (ANAFORCAL), Aix-en-Provence, France; [e]the French Committee of Support (Comite de Soutien de l'Allergologie), Clermont-Ferrand, France; [f]the French Trade Union of Allergists (SNAF), Tarbes, France; and [g]the Trade Union of Allergists (ANAICE), Tours, France. E-mail: Frederic.deblay@chru-strasbourg.fr.

*APSI group: I. Bosse, La Rochelle; J. C. Farouz, Bordeaux, ANAICE, France; M. Epstein, C. Martens, Paris, SNAF, France; P. Demoly, Inserm U657, CHU de Montpellier, Montpellier; A. Didier, CHU de Toulouse, Toulouse, French Society of Allergology.

Disclosure of potential conflict of interest: F. de Blay and A. de Laval have received research support from Stallergènes and ALK-Abelló. The rest of the authors declare that they have no relevant conflicts of interest.

REFERENCES

1. Slater JE, Menzies SL, Bridgewater J, Mosquera A, Zinderman CE, Ou AC, et al. The US Food and Drug Administration review of the safety and effectiveness of nonstandardized allergen extracts. J Allergy Clin Immunol 2012;129:1014-9.
2. Slater JE. Standardized allergen vaccines in the United States. Clin Allergy Immunol 2008;21:273-81.
3. Directive 2001/83/EC of the European Parliament and of the Council of 6 November 2001 on the Community code relating to medicinal products for human use. Available at: http://eur-lex.europa.eu/LexUriServ/LexUriServ.do?uri=OJ:L:2001:311:0067:0128:EN:PDF. Accessed July 2, 2009.
4. Lorenz AR, Lüttkopf D, Seitz R, Vieths S. The regulatory system in Europe with special emphasis on allergen products. Int Arch Allergy Immunol 2008;147:263-75.
5. Summary of the response to the questionnaire marketing authorization of allergen products in Europe sent to national regulatory agencies. Arb Paul Ehrlich Inst Bundesamt Sera Impfstoffe Frankf A M 2006;(95):43-4.
6. Kaul S, May S, Lüttkopf D, Vieths S. Regulatory environment for allergen-specific immunotherapy. Allergy 2011;66:753-64.
7. Ministère de la santé et des solidarités. Décret n° 2004-188 du 23 février 2004 relatif aux allergènes préparés spécialement pour un seul individu et modifiant le code de la santé publique. OJ 200;50:4101 texte n° 30.
8. European Medicine Agency (EMEA), Committee for Medicinal Products for Human Use (CHMP) and Biologics Working Party (BWP): guideline on allergen products: production and quality issues, 2007; EMEA/CHMP/BWP/304831/2007. Available at: http://www.pei.de/cln_227/nn_162408/EN/medicinal-products/allergens/allergens-node.html?__nnn=true Accessed May 1, 2012.
9. Larsen JN, Dreborg S. Standardization of allergen extracts. Methods Mol Med 2008;138:133-45.

Available online January 30, 2013.
http://dx.doi.org/10.1016/j.jaci.2012.11.003

Common variable immunodeficiency classification by quantifying T-cell receptor and immunoglobulin κ-deleting recombination excision circles

To the Editor:

Common variable immunodeficiency (CVID) is the most frequent primary immunodeficiency associated with hypogammaglobulinemia and other various clinical manifestations. CVID was originally reported to be a disease primarily caused by defective B-cell function, with defective terminal B-cell differentiation rendering B cells unable to produce immunoglobulin. However, combined immunodeficiency (CID) involving both defective B and T cells is often misdiagnosed as CVID.[1] Indeed, one study reported that $CD4^+$ T-cell numbers were decreased in 29% of 473 patients with CVID[2]; similarly, another study found that naive T-cell numbers were markedly reduced in 44% (11/25) of patients with CVID.[3] These observations indicated that a subgroup of patients with clinically diagnosed CVID is T-cell deficient. Consistently, some patients with CVID have complications that might be related to T-cell deficiency, including opportunistic infections, autoimmune diseases, and malignancies, which is similar to that observed in patients with CID.[1,4] Therefore identifying novel markers to better classify CVID and distinguish CID from CVID will be required to best manage medical treatment for CVID.

We recently performed real-time PCR-based quantification of T-cell receptor excision circles (TREC) and signal joint immunoglobulin κ-deleting recombination excision circles (KREC) for mass screening of severe combined immunodeficiency (SCID)[5] and B-lymphocyte deficiency[6] in neonates. TREC and KREC are associated with T-cell and B-cell neogenesis, respectively.[7] Here we retrospectively report that TREC and KREC are useful for classifying patients with clinically diagnosed CVID.

Hypogammaglobulinemic patients (n = 113) were referred to our hospital for immunodeficiency from 2005-2011, and the following patients were excluded from the CVID pool by estimating their SCID genes based on clinical manifestations and lymphocyte subset analysis: 18 patients with SCID diagnoses; 14 patients less than 2 years of age (transient infantile hypogammaglobulinemia); 10 patients with IgM levels of greater than 100 mg/dL (hyper-IgM syndrome); 26 patients with diseases other than CVID caused by known gene alterations (10 with X-linked agammaglobulinemia and 11 with hyper-IgM syndrome

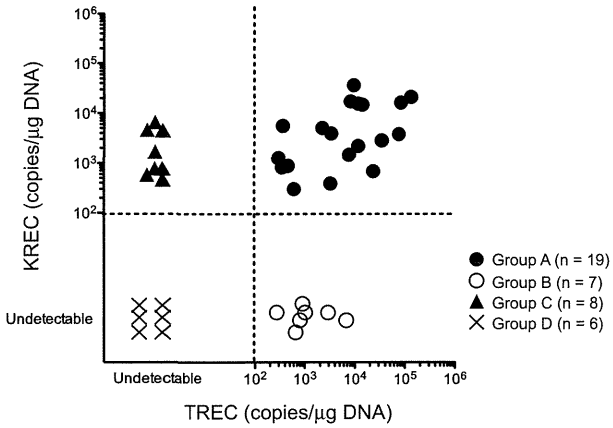

FIG 1. Quantifying TREC and KREC classifies patients with CVID into 4 groups. Patients with CVID were classified as follows: TREC(+)/KREC(+), group A (19 patients); TREC(+)/KREC(−), group B (7 patients); TREC(−)/KREC(+), group C (8 patients); and TREC(−)/KREC(−), group D (6 patients). *Undetectable,* Less than 100 copies/μg DNA.

[*CD40L* or *AICDA* mutated]), (2 with DiGeorge syndrome, and 3 with *FOXP3*, *IKBKG*, or *6p* deletions); and 5 patients with drug-induced hypogammaglobulinemia. The remaining 40 patients with decreased IgG (≥2 SDs below the mean for age), IgM, and/or IgA levels, as well as absent isohemagglutinins, poor response to vaccines, or both were included in this study as patients with CVID and analyzed for TREC/KREC levels, retrospectively.

Ages of patients with CVID ranged from 2 to 52 years (median age, 15.5 years). The sex ratio of the patients was 21 male/19 female patients. Serum IgG, IgA, and IgM levels were 370 ± 33 mg/dL (0-716 mg/dL), 30 ± 7 mg/dL (1-196 mg/dL), and 40 ± 6 mg/dL (2-213 mg/dL), respectively. TREC and KREC quantification was performed by using DNA samples extracted from peripheral blood, as reported previously.[5,6] Clinical symptoms were then assessed retrospectively. The study protocol was approved by the National Defense Medical College Institutional Review Board, and written informed consent was obtained from adult patients or parents of minor patients in accordance with the Declaration of Helsinki.

Based on TREC and KREC copy numbers, the 40 patients with CVID were classified into 4 groups (groups A, B, C, and D; Fig 1). Comparing lymphocyte subsets, $CD3^+$ T-cell numbers were similar among groups A, B, and D but were significantly lower in group C ($P < .05$; group A, 1806 ± 204 cells/μL; group B, 1665 ± 430 cells/μL; group C, 517 ± 124 cells/μL; and group D, 1425 ± 724 cells/μL; $P = .0019$, Tukey multiple comparison test based on 1-way ANOVA). $CD3^+CD4^+CD45RO^+$ memory T-lymphocyte percentages in groups B, C, and D were significantly higher than those in group A ($P < .0001$; group A, 37% ± 16%; group B, 67% ± 13% [$P = .0006$]; group C, 92% ± 8.2% [$P < .0001$]; and group D: 83% ± 14% [$P < .0001$]; see Fig E1 in this article's Online Repository at www.jacionline.org); additionally, the percentages of these cells in groups C and D were higher than in group B ($P = .0115$). These results indicate that group C and D patients have markedly decreased $CD4^+CD45RA^+$ naive T-cell counts than group A patients and that counts in group B are also significantly decreased, although less so than in groups C or D, which is consistent with a report showing lower TREC copy numbers in $CD4^+CD45RO^+$ cells. Some patients in groups B, C, and D exhibited normal $CD4^+CD45RO^+$ percentages, although TREC levels, KREC levels, or both decreased. This discrepancy indicates that TREC/KREC levels could be independent markers to determine the patient's immunologic status in addition to $CD4^+CD45RA^+$; the reasons underlying the discrepancy between $CD4^+CD45RA^+$ and TREC/KREC levels remain unsolved.

$CD19^+$ B-cell numbers in group A were significantly higher ($P < .05$) than those in groups B and D (group A, 269 ± 65 cells/μL; group B, 35 ± 16 cells/μL; group C, 60 ± 11 cells/μL; and group D, 29 ± 16 cells/μL; $P = .0001$). However, B-cell subpopulations, including $CD27^-$, IgD^+CD27^+, and IgD^-CD27^+ cells, were not significantly different among the groups. Standardizing KREC copy numbers for each patient by dividing their $CD19^+$ by their $CD27^+$ percentages revealed the same patient classification as that shown in Fig 1 (data not shown), indicating that the original classification was independent of $CD19^+$ B-cell or $CD27^+$ memory B-cell percentages.

Because TREC and KREC levels decrease with age (see Fig E2 in this article's Online Repository at www.jacionline.org)[5,6] and age distribution was wide in this study, we compared patients' ages among groups at the time of analysis to determine whether classification was associated with age. TREC/KREC-based classification was independent of both age and sex because age distribution was not significantly different among groups ($P > .05$; group A, 12.7 ± 2.3 years [2-30 years]; group B, 23.4 ± 4.2 years [6-39 years]; group C, 21.5 ± 6.1 years [4-52 years]; and group D, 25.5 ± 4.4 years [15-46 years]; data not shown) nor was male/female sex ratio (overall, 21/19; group A, 10/9; group B, 2/5; group C, 5/3; and group D, 4/2; $P = .4916$, χ^2 test; data not shown).

We next evaluated whether any correlation existed between TREC/KREC-based classification and clinical symptoms in each patient group. All patients in the study had been treated with intravenous immunoglobulin (IVIG) substitution at the time of analysis. We found that the cumulative events of complications (opportunistic infections, autoimmune diseases, and malignancies) per 10 patient-years were highest in group D (0.98 events/10 patient-years), followed by group C (0.63 events/10 patient-years), group B (0.30 events/10 patient-years), and group A (0.04 events/10 patient-years), where events in groups D and C were significantly higher than group A (group A vs group D, $P = .0022$; group A vs group C, $P = .0092$; group A vs group B, $P = .0692$; Fig 2). Furthermore, we found similar results when evaluating only patients 19 years old or older for group D (1.01 events/10 patient-years), group C (0.56 events/10 patient-years), group B (0.32 events/10 patient-years), and group A (0.06 events/10 patient-years; group A vs group D, $P = .0074$; group A vs group C, $P = .0407$; group A vs group B, $P = .1492$; data not shown). Categorizing patients by using several different previously reported CVID classifications (focused primarily on separating patients based on levels of circulating B-cell subsets), we found that no classification scheme showed any significant event increases in any particular group (see Fig E3 in this article's Online Repository at www.jacionline.org). Assessing longitudinal cumulative opportunistic infection incidence among the groups, group D and C values were significantly higher than in group A (see Fig E4, A, in this article's Online Repository at www.jacionline.org; $P = .0059$). Autoimmune and malignant diseases ($P = .5168$ and $P = .6900$, respectively) were observed in groups B and D but not in group A (see Fig E4, *B* and *C*). Cumulative events were significantly different between groups ($P = .0313$, log-rank test; group A, 5.3% and 5.3%; group B, 14.3% and

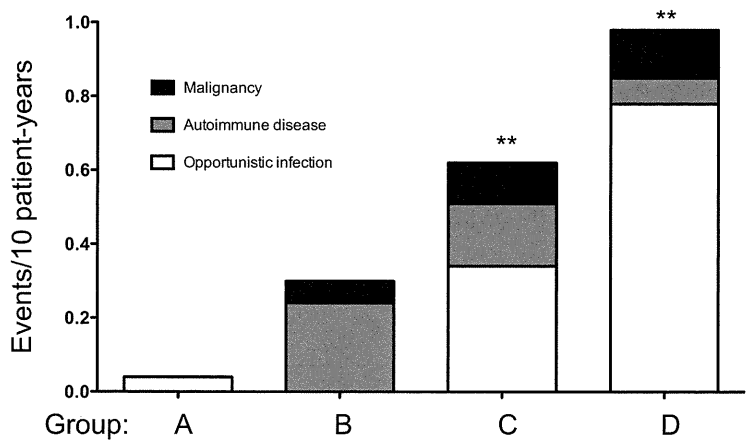

FIG 2. Cumulative incidence of complication events per 10 patient-years differs among groups. Opportunistic infections, autoimmune diseases, and malignancies were evaluated for each patient group. Complication incidences in group D (0.98 events/10 patient-years), group C (0.63 events/10 patient-years), and group B (0.30 events/10 patient-years) were higher than in group A (0.04 events/10 patient-years). Group A versus group D: $^{**}P = .0022$; group A versus C: $^{**}P = .0092$; group A vs group B: $P = .0692$.

57.1%; group C, 27.1% and 63.5%; and group D, 33.3% and 83.3% at 10 and 30 years of age, respectively; see Fig E4, *D*). One patient in group D died of *Pneumocystis jirovecii* pneumonia, and 2 other patients in the same group received hematopoietic stem cell transplantation after complications caused by EBV-related lymphoproliferative disorder.

Assessing these data, TREC/KREC-based classification matches clinical outcomes. Because group D patients exhibited the most frequent complications (opportunistic infections, autoimmune diseases, and malignancies), they could receive a diagnosis of CID based on these symptoms. If they are indeed determined to have CID, then TREC/KREC analysis is helpful to distinguish between CID and CVID. Their TREC(−)/KREC(−) phenotype might relate to defective V(D)J recombination in T- and B-cell development[8] because patients with B-negative SCID (*RAG1*, *RAG2*, *Artemis*, and *LIG4*), as well as patients with ataxia-telangiectasia (AT) and Nijmegen breakage syndrome (NBS; see Fig E5 in this article's Online Repository at www.jacionline.org),[5,6] were also negative for both TREC and KREC; it is intriguing to speculate that an unknown V(D)J recombination gene or genes is responsible. As for treatment, hematopoietic stem cell transplantation should be considered the preferred treatment to "cure" group D patients, as reported in patients with severe CVID/CID, because event-free survival is poor.[9]

In contrast to group D patients, TREC(+)/KREC(+) group A patients treated with IVIG substitution therapy remained healthy. One possible explanation is that these patients harbor defects only in terminal B-cell differentiation, but not in T cells, and represent typical patients with CVID, as originally reported.

Group C patients had a high frequency of both opportunistic infections and malignancies, suggesting that these TREC(−) patients have T-cell defects. Although group C patients had a similar TREC/KREC pattern to patients with SCID with B cells (*IL2RG* and *JAK3*; see Fig E5, *A*), they do not fulfill the European Society for Immunodeficiencies criteria for SCID, and no mutation was identified in the SCID genes estimated from clinical manifestation and lymphocyte subset analysis. However, from our data, they would likely benefit from undergoing similar treatment to patients with SCID or CID to prevent these complications.

Although opportunistic infections were rare in group B patients, autoimmune diseases were often observed. This is consistent with this group being TREC(+)/KREC(−) and the idea that balance between T and B cells is important to prevent autoimmune diseases in patients with CVID.[1] Intriguingly, a group of patients with AT and NBS were also TREC(+)/KREC(−) (see Fig E4, *B*), which is similar to group B patients. Additionally, $CD45RA^{+}CD4^{+}$ naive T-cell numbers were reduced in most group B patients, which is similar to the phenotype exhibited by patients with AT and NBS. This finding raises the possibility that although some group B patients are also T-cell deficient, as well as B-cell deficient, and should be treated similarly to patients with CID, other patients have only B-cell deficiency and are effectively treated with IVIG substitution therapy.

By analyzing a large CVID patient cohort, the overall survival rate of patients with more than 1 complication was worse than that for patients without other complications.[4] Our findings indicate that low TREC levels, KREC levels, or both are useful markers that correlate well with the overall survival rate in patients with CVID. Therefore we conclude that TREC and KREC are useful markers to assess the clinical severity and pathogenesis of each patient with CVID and to distinguish CID from CVID. Thus patient classification based on TREC/KREC levels would provide a helpful tool for deciding on an effective treatment plan for each patient with CVID.

We thank the following doctors who contributed patient data to this study: Satoshi Okada, Kazuhiro Nakamura, Masao Kobayashi, Tomoyuki Mizukami, Yoshitora Kin, Hironobu Yamaga, Shinsuke Yamada, Kazuhide Suyama, Chihiro Kawakami, Yuko Yoto, Kensuke Oryoji, Ayumu Itoh, Takao Tsuji, Daisuke Imanishi, Yutaka Tomishima, Minako Tomiita, Kaori Sasaki, Akira Ohara, Hanako Jimi, Mayumi Ono, Daisuke Hori, Yuichi Nakamura, Yoshitoshi Otsuka, Toshiyuki Kitoh, Toshio Miyawaki, Akihiko Maeda, Terumasa Nagase, Takahiro Endo, Yoshiaki Shikama, Mikiya Endo, Satoru Kumaki, Lennart Hammarström, Janine Reichenbach, and Reinhard Seger. We also thank Professor Junichi Yata for critical reading and Ms Kaori Tomita, Ms Kimiko Gasa, and Ms Atsuko Kudo for their skillful technical assistance.

Chikako Kamae, MD[a]
Noriko Nakagawa, MD, PhD[a]
Hiroki Sato, MS[b]
Kenichi Honma, MD[a]
Noriko Mitsuiki, MD[c,d]
Osamu Ohara, PhD[c]
Hirokazu Kanegane, MD, PhD[e]
Srdjan Pasic, MD, PhD[f]
Qiang Pan-Hammarström, MD, PhD[g]
Menno C. van Zelm, PhD[h]
Tomohiro Morio, MD, PhD[d]
Kohsuke Imai, MD, PhD[a]
Shigeaki Nonoyama, MD, PhD[a]

From the Departments of [a]Pediatrics and [b]Preventive Medicine and Public Health, National Defense Medical College, Saitama, Japan; [c]the Department of Human Genome Research, Kazusa DNA Research Institute, Chiba, Japan; [d]the Department of Pediatrics, Tokyo Medical and Dental University, Tokyo, Japan; [e]the Department of Pediatrics, University of Toyama, Toyama, Japan; [f]the Department of Immunology, Mother and Child Health Institute, Medical Faculty, University of Belgrade, Belgrade, Serbia; [g]the Department of Laboratory Medicine, Karolinska Institute, Karolinska University Hospital, Huddinge, Stockholm, Sweden; and [h]the Department of Immunology, Erasmus MC, University Medical Center, Rotterdam, The Netherlands. E-mail: kimai.ped@tmd.ac.jp.

Supported in part by grants from the Ministry of Defense; the Ministry of Health, Labour, and Welfare; and the Ministry of Education, Culture, Sports, Science, and Technology.

Disclosure of potential conflict of interest: The authors declare that they have no relevant conflicts of interest.

REFERENCES

1. Yong PFK, Thaventhiran JED, Grimbacher B. "A rose is a rose is a rose," but CVID is not CVID. common variable immune deficiency (CVID), what do we know in 2011? Adv Immunol 2011;111:47-107.
2. Resnick ES, Moshier EL, Godbold JH, Cunningham-Rundles C. Morbidity and mortality in common variable immune deficiency over 4 decades. Blood 2012;119: 1650-7.
3. Moratto D, Gulino AV, Fontana S, Mori L, Pirovano S, Soresina A, et al. Combined decrease of defined B and T cell subsets in a group of common variable immunodeficiency patients. Clin Immunol 2006;121:203-14.
4. Chapel H, Lucas M, Lee M, Bjorkander J, Webster D, Grimbacher B, et al. Common variable immunodeficiency disorders: division into distinct clinical phenotypes. Blood 2008;112:277-86.
5. Morinishi Y, Imai K, Nakagawa N, Sato H, Horiuchi K, Ohtsuka Y, et al. Identification of severe combined immunodeficiency by T-cell receptor excision circles quantification using neonatal Guthrie cards. J Pediatr 2009;155:829-33.
6. Nakagawa N, Imai K, Kanegane H, Sato H, Yamada M, Kondoh K, et al. Quantification of κ-deleting recombination excision circles in Guthrie cards for the identification of early B-cell maturation defects. J Allergy Clin Immunol 2011;128:223-5.e2.
7. van Zelm MC, Szczepanski T, Van Der Burg M, Van Dongen JJM. Replication history of B lymphocytes reveals homeostatic proliferation and extensive antigen-induced B cell expansion. J Exp Med 2007;204:645-55.
8. Verbsky JW, Baker MW, Grossman WJ, Hintermeyer M, Dasu T, Bonacci B, et al. Newborn screening for severe combined immunodeficiency; the Wisconsin experience (2008-2011). J Clin Immunol 2012;32:82-8.
9. Rizzi M, Neumann C, Fielding AK, Marks R, Goldacker S, Thaventhiran J, et al. Outcome of allogeneic stem cell transplantation in adults with common variable immunodeficiency. J Allergy Clin Immunol 2011;128:1371-2.

Available online December 28, 2012.
http://dx.doi.org/10.1016/j.jaci.2012.10.059

Homing frequency of human T cells inferred from peripheral blood depletion kinetics after sphingosine-1-phosphate receptor blockade

To the Editor:

Naive and central memory (CM) T cells home through lymph nodes (LNs), whereas T cells with an effector memory (EM) phenotype preferentially screen peripheral tissues in search of cognate antigen.[1] LN entry and egress are distinct and highly regulated processes mediated by an orchestrated interplay of chemokines/chemokine receptors and adhesion molecules.[2] Interaction of peripheral node addressins with L-selectin on T cells allows tethering/rolling along high endothelial venules (HEVs).[2] Interaction of the chemokine receptor CCR7 with its ligands CCL19/CCL21 and CXCR4 with CXCL12 then mediates firm adhesion to HEVs through high-affinity interactions of lymphocyte function–associated antigen 1 and intercellular adhesion molecule 1, permitting transmigration of T cells across the HEV cell layer.[2] Within the LNs, T-cell migration is directed through T-cell zones toward the cortical sinuses.[3] A sphingosine-1-phosphate (S1P) gradient established across the endothelial cells of the cortical sinuses is directing LN egress of T cells through efferent lymph back to the peripheral blood circulation.[4] Acting as a functional antagonist on the S1P receptor, the pharmacologic compound fingolimod, which has shown efficacy in the treatment of multiple sclerosis (MS), blocks this egress.[4,5] As a consequence, in fingolimod-treated subjects naive and CM T cells are trapped in LNs and reduced in the blood circulation.[6]

Here, by studying depletion kinetics of T cells in the blood of *de novo* fingolimod-exposed subjects in combination with *in vitro* migration experiments, homing frequencies and LN access hierarchy between T-cell subsets were derived indirectly. First, we defined the effect of *de novo* fingolimod exposure on the number of circulating $CD4^+$ and $CD8^+$ phenotypic T-cell subsets in patients with MS during a 6-hour observation period (hourly measurements, 1 time before and 6 times after drug exposure) by using flow cytometry (detailed information on patients and methods is provided in the Methods section and Table E1 in this article's Online Repository at www.jacionline.org). In fingolimod-treated subjects, 6 hours after the first drug dose, numbers of $CD4^+$ T-cell subsets with an LN homing phenotype (ie, naive and CM T cells) were significantly reduced (Fig 1, *A* [representative example; absolute cell counts], and Fig 1, *B* [pooled data; proportional change]). Intriguingly, the kinetics of reduction differed between phenotypic naive (CD62 ligand [CD62L]–positive $CD45RA^+$) and CM ($CD62L^+CD45RA^-$) $CD4^+$ T cells. Specifically, compared with baseline measurements, naive $CD4^+$ T-cell counts started to decrease earlier than CM $CD4^+$ T-cell counts (2 vs 5 hours after fingolimod exposure; Fig 1, *B*). In $CD8^+$ T cells, contrasting $CD4^+$ T cells, only naive ($CD62L^+CD45RA^+$) $CD8^+$ T-cell counts decreased significantly (after 3 vs 2 hours in naive $CD4^+$ T cells) after the first dose of fingolimod (Fig 1, *C* [representative example; absolute cell counts], and Fig 1, *D* [pooled data; proportional change]).

On the basis of these *ex vivo* depletion kinetics, *in vitro* chemotaxis experiments were performed, as described in the Methods section in this article's Online Repository. In a transwell system spontaneous migration of bulk $CD4^+$ and $CD8^+$ T cells was comparably low in healthy control subjects and untreated patients with MS (and was further decreased in the presence of fingolimod; see Fig E1 in this article's Online Repository at www.jacionline.org). Gradients of CXCL12, CCL19, and CCL21 mediated a clear increase in migration of bulk $CD4^+$ and $CD8^+$ T cells from healthy control subjects and untreated patients with MS, which was not significantly influenced by fingolimod (see Fig E1). Dot plot distribution (as a percentage) of migrated versus nonmigrated, phenotypic naive, CM, EM, and (for $CD8^+$ T cells) CD45RA re-expressing EM cells (EMRA) was then compared between control cells (spontaneous migration) and cells that migrated toward CXCL12, CCL19, or CCL21. An example of CXCL12-mediated changes in the

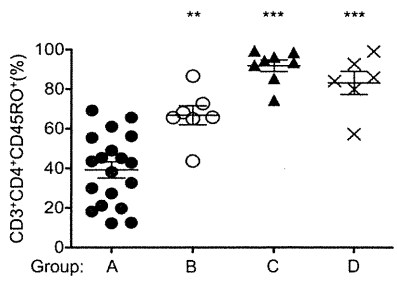

FIG E1. $CD45RO^+CD3^+CD4^+$ T-cell frequency within $CD4^+CD3^+$ lymphocytes was analyzed among groups. $CD45RO^+CD3^+CD4^+$ lymphocyte counts were significantly higher in groups B, C, and D compared with those in group A ($P < .0001$). Group A: 37% ± 16%; group B: 67% ± 13% (**$P < .01$); group C: 92% ± 8.2% (***$P < .001$); and group D: 83% ± 14% (***$P < .001$).

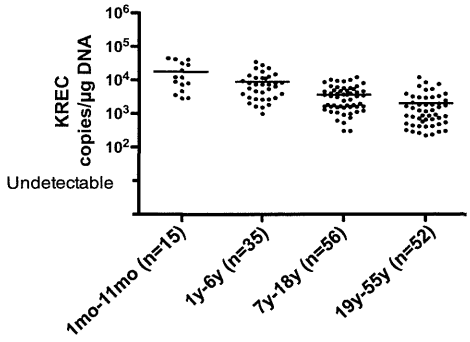

mean:	17.9	8.9	3.6	2.0	
max:	442	349	12.1	12.0	x10^3 copies/µg DNA
min:	2.8	0.99	0.29	0.22	

FIG E2. KREC levels were analyzed in genomic DNA samples extracted from peripheral blood of control subjects at different age groups (n = 158; age range, 1 month to 55 years). KREC levels were significantly higher in infants (17.9 ± 3.9 × 10^3 copies/µg DNA) compared with other children's age groups (8.9 ± 1.3 × 10^3 copies/µg DNA in the 1- to 6-year-old group and 3.6 ± 3.8 × 10^3 copies/µg DNA in the 7- to 18-year-old group) and adults (2.0 ± 3.3 × 10^3 copies/µg DNA; $P < .0001$).

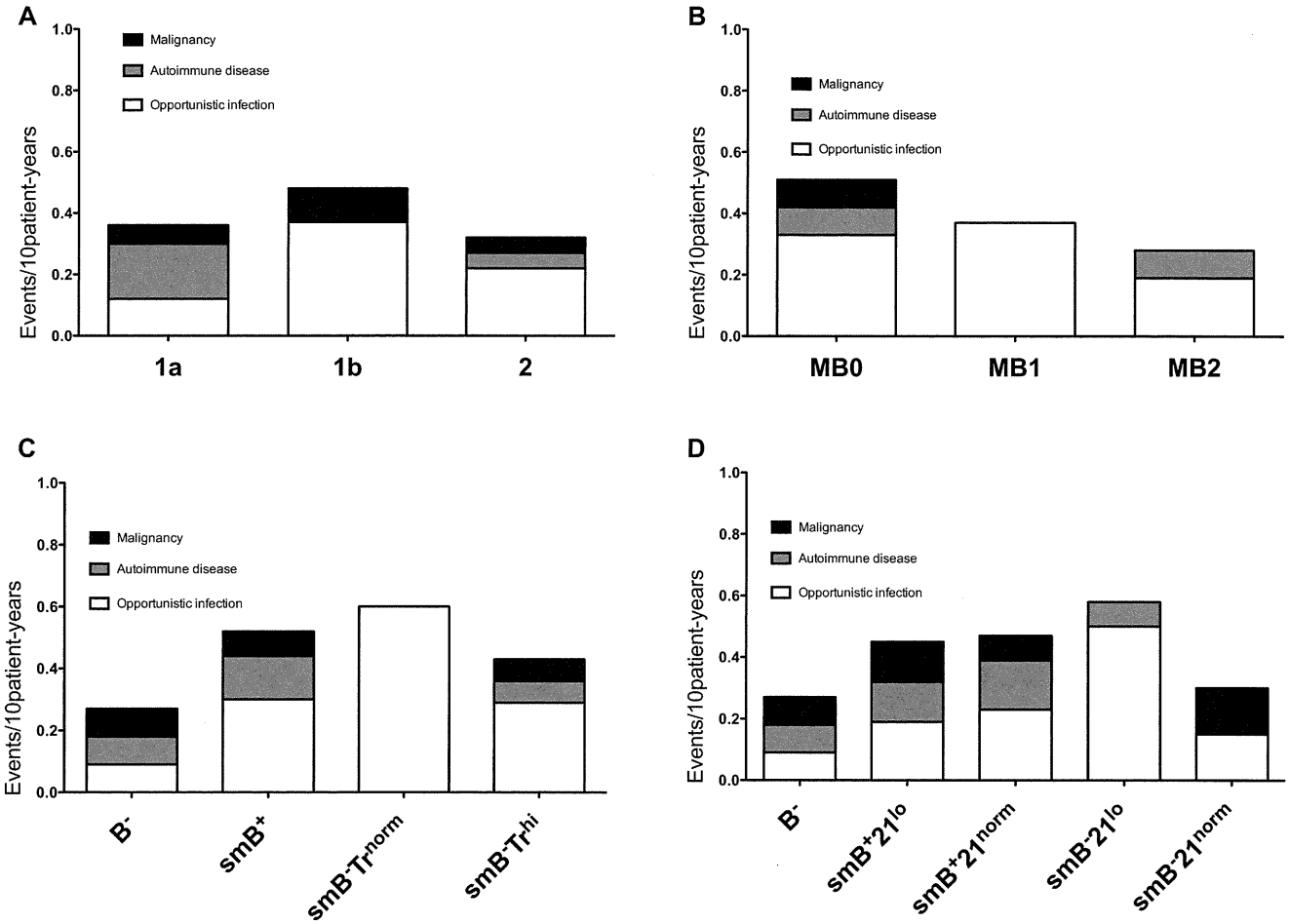

FIG E3. Patients were classified in the following way and analyzed for cumulative incidence of complications: **A,** Freiburg; **B,** Paris; and **C,** EUROclass classifications, according to $CD38^{hi}IgM^{hi}$ transitional B cells (Fig E3, *A-C*) or $CD21^{low}$ B cells **(D)**. Five patients were excluded from the Freiburg and Paris classifications because of decreased B-cell numbers (<1%). Additionally, we excluded 4 patients in the Freiburg classification, 1 patient in the Paris classification, and 4 patients in the EUROclass classification for transitional B cells and 8 in the EUROclass classification for $CD21^{low}$ B cells because of lack of data. The following cumulative events/10 patient-years were found. Freiburg classification: 1a, 0.36; 1b, 0.48; 2, 0.32. Paris classification: MB0, 0.50; MB1, 0.37; MB2, 0.28. EUROclass classification according to transitional B cells: B^-, 0.27; smB^+, 0.52; smB^-Tr^{norm}, 0.60; smB^-Tr^{high}, 0.43. EUROclass classification according to $CD21^{lo}$ B cells: B^-, 0.27; smB^+21^{lo}, 0.45; smB^+21^{norm}, 0.47; smB^-21^{lo}, 0.58; smB^-21^{norm}, 0.30. No classification showed any significantly increased events in any particular group according to calculated *P* values, as follows—Freiburg classification: 1a vs 2 = .898, 1b vs 2 = .479, 1a vs 1b = .838; Paris classification: MB0 vs MB2 = .179, MB1 vs MB2 = .654, MB0 vs MB1 = .764; EUROclass classification according to transitional B cells: B^- vs smB^+ = .298, smB^-Tr^{norm} vs smB^+ = .809, smB^-Tr^{hi} vs smB^+ = .702, smB^-Tr^{hi} vs smB^-Tr^{norm} = .641, smB^-Tr^{norm} vs B^- = .329, smB^-Tr^{hi} vs B^- = .508; EUROclass classification according to $CD21^{lo}$ B cells: B^- vs smB^+21^{norm} = .443, smB^+21^{lo} vs smB^+21^{norm} = .930, smB^-21^{lo} vs smB^+21^{norm} = .695, smB^-21^{norm} vs smB^+21^{norm} = .575, B^- vs smB^-21^{norm} = .926, smB^+21^{lo} vs smB^-21^{norm} = .609, smB^-21^{lo} vs smB^-21^{norm} = .399, B^- vs smB^+21^{lo} = 0.474, B^- vs smB^-21^{lo} = 0.270, smB^+21^{lo} vs smB^-21^{lo} = 0.618.

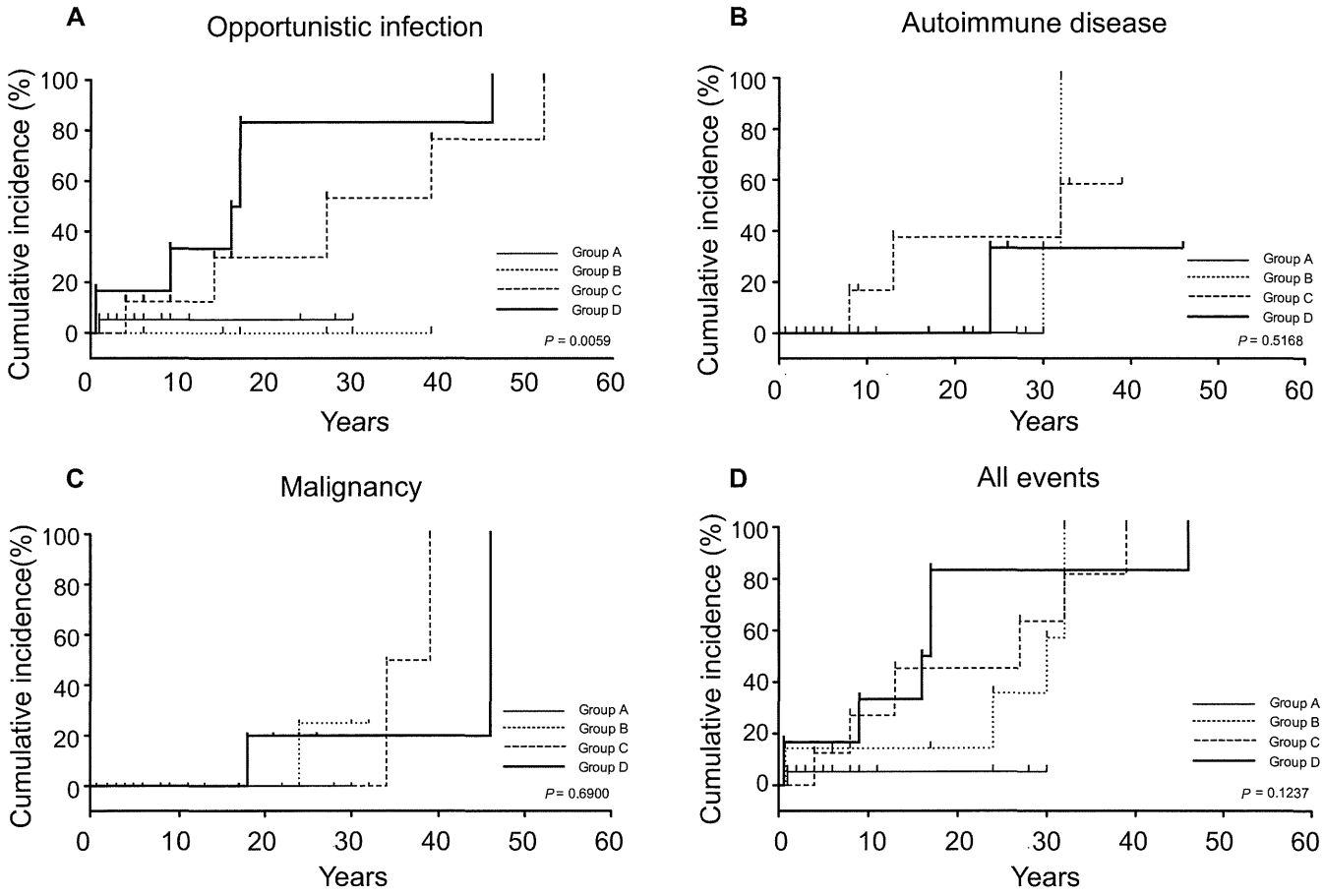

FIG E4. Comparing longitudinal cumulative incidence of complication events among groups. Cumulative incidence was estimated separately and longitudinally by using the Kaplan-Meier method and statistically compared between groups by using the log-rank test. The cumulative incidence of opportunistic infections **(A)**, autoimmune diseases **(B)**, malignancies **(C)**, and all events **(D)** is shown.

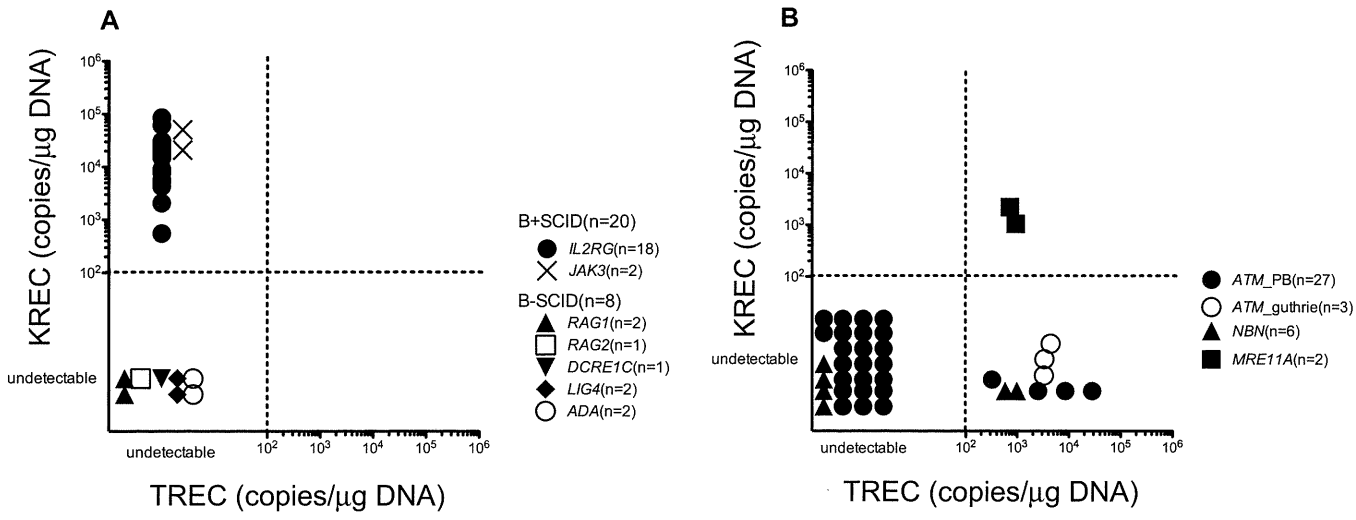

FIG E5. TREC and KREC quantification classifies patients with SCID, AT, NBS, or ataxia-telangiectasia–like disease *(ATLD)* into 4 groups. **A,** Patients with B^+SCID (n = 20) were classified as group C, and patients with B^-SCID (n = 8) were classified as group D; these patients were included in the previous studies.[5,6] **B,** Although most patients with AT (n = 23) and patients with NBS (n = 4) were classified as group D, TRECs were detected in peripheral blood samples (n = 4 in patients with AT and n = 2 in patients with NBS) and neonatal Guthrie cards (n = 3) of some patients with AT, who were classified as group B. Patients with ATLD with *MRE11A* mutations were classified as group A.

THE JOURNAL OF BIOLOGICAL CHEMISTRY VOL. 288, NO. 11, pp. 7451–7466, March 15, 2013

Depletion of Molecular Chaperones from the Endoplasmic Reticulum and Fragmentation of the Golgi Apparatus Associated with Pathogenesis in Pelizaeus-Merzbacher Disease*

Received for publication, November 13, 2012, and in revised form, January 23, 2013 Published, JBC Papers in Press, January 23, 2013, DOI 10.1074/jbc.M112.435388

Yurika Numata[‡§], Toshifumi Morimura[‡¶], Shoko Nakamura[‡], Eriko Hirano[‡], Shigeo Kure[§], Yu-ich Goto[‡], and Ken Inoue[‡1]

From the [‡]Department of Mental Retardation and Birth Defect Research, National Institute of Neuroscience, National Center of Neurology and Psychiatry (NCNP), 4-1-1 Ogawahigashi-machi, Kodaira-shi, Tokyo 187-8502, the [§]Department of Pediatrics, Tohoku University School of Medicine, 1-1 Seiryomachi, Aobaku, Sendai 980-8574, and the [¶]Unit for Neurobiology and Therapeutics, Molecular Neuroscience Research Center, Shiga University of Medical Science, Seta-Tsukinowa-cho, Otsu, Shiga 520-2192, Japan

Background: Mutations of proteolipid protein 1 (*PLP1*) induce endoplasmic reticulum (ER) stress.
Results: PLP1 mutants deplete some chaperones from the ER and induce fragmentation of the Golgi apparatus (GA).
Conclusion: These changes affect clinical pathology in disease-causing mutations of *PLP1*.
Significance: This work provides a novel insight involving global changes of organelles in pathogenesis of ER stress-related diseases.

Missense mutations in the proteolipid protein 1 (*PLP1*) gene cause a wide spectrum of hypomyelinating disorders, from mild spastic paraplegia type 2 to severe Pelizaeus-Merzbacher disease (PMD). Mutant PLP1 accumulates in the endoplasmic reticulum (ER) and induces ER stress. However, the link between the clinical severity of PMD and the cellular response induced by mutant PLP1 remains largely unknown. Accumulation of misfolded proteins in the ER generally leads to up-regulation of ER chaperones to alleviate ER stress. Here, we found that expression of the PLP1-A243V mutant, which causes severe disease, depletes some ER chaperones with a KDEL (Lys-Asp-Glu-Leu) motif, in HeLa cells, MO3.13 oligodendrocytic cells, and primary oligodendrocytes. The same PLP1 mutant also induces fragmentation of the Golgi apparatus (GA). These organelle changes are less prominent in cells with milder disease-associated PLP1 mutants. Similar changes are also observed in cells expressing another disease-causing gene that triggers ER stress, as well as in cells treated with brefeldin A, which induces ER stress and GA fragmentation by inhibiting GA to ER trafficking. We also found that mutant PLP1 disturbs localization of the KDEL receptor, which transports the chaperones with the KDEL motif from the GA to the ER. These data show that PLP1 mutants inhibit GA to ER trafficking, which reduces the supply of ER chaperones and induces GA fragmentation. We propose that depletion of ER chaperones and GA fragmentation induced by mutant misfolded proteins contribute to the pathogenesis of inherited ER stress-related diseases and affect the disease severity.

A number of inherited human diseases are caused by missense mutations. These mutations in the membrane and secretary proteins often lead to improper protein folding and accumulation in the endoplasmic reticulum (ER),[2] resulting in an induction of ER stress. In cells under ER stress, accumulation of mutant proteins in the ER activates the unfolded protein response (UPR), which initiates a block in translation, increases retrotranslocation and degradation of ER-localized proteins, and bolsters the protein-folding capacity of the ER (1, 2). Through these processes, the UPR functions as a cellular quality control system that essentially protects cells from the toxicity of accumulated proteins in the ER. The UPR is activated by three distinct pathways, activating transcription factor 6 (ATF6), inositol-requiring kinase 1 (IRE1), and protein kinase-like ER kinase (3), all of which are negatively regulated by interaction with the 78-kDa glucose-regulated protein (GRP78, also referred to as BiP/HSPA5). On accumulation of unfolded protein, GRP78 binds to unfolded proteins and dissociates from

* This work was supported in part by grants from the Health and Labor Sciences Research Grants, Research on Intractable Diseases H24-Nanchitou-Ippan-072 (to K. I.), a grant from Takeda Science Foundation (to K. I.), and Grants-in-Aid for Scientific Research from the Ministry of Education, Culture, Sports, Science and Technology, Japan, KAKENHI: 21390103 and 23659531 (to K. I.) and 23580417 (to T. M.).
[1] To whom correspondence should be addressed. Tel.: 81-42-346-1713; Fax: 81-42-346-1743; E-mail: kinoue@ncnp.go.jp.

[2] The abbreviations used are: ER, endoplasmic reticulum; PLP1, proteolipid protein 1; PMD, Pelizaeus-Merzbacher disease; msd, myelin synthesis deficit; SPG2, spastic paraplegia type 2; msd, myelin synthesis deficit; GA, Golgi apparatus; PDI, protein-disulfide isomerase; CALR, calreticulin; GRP78, glucose-regulated protein of 78 kDa; CANX, calnexin; MBP, myelin basic protein; UPR, unfolded protein response; ATF6, activating transcription factor 6; IRE1, inositol-requiring kinase 1; XBP1, X-box protein 1; CHOP, C/EBP homologous protein; ALS, amyotrophic lateral sclerosis; MPZ, myelin protein zero; PMP22, peripheral myelin protein 22; CMT, Charcot-Marie-Tooth disease; SC, spinal cords; TUNEL, terminal deoxynucleotidyl transferase dUTP nick end labeling; MGC, mixed glial culture; BFA, brefeldin A; MOG, myelin oligodendrocyte glycoprotein; GFP, green fluorescent protein; luc, luciferase; Rluc, *Renilla* luciferase; Igκ, immunoglobulin κ light chain; Cluc, cytoplasmic luciferase; DMSO, dimethyl sulfoxide.

the ER stress sensors, which trigger the UPR (3). ATF6 induces transcription of major ER chaperones and X box-binding protein 1 (*XBP1*) (4). The endonuclease activity of IRE1 splices *XBP1* (5), which functions as a transcription factor that drives the expression of UPR-related genes (4). The ATF6 and IRE1-XBP1 axes promote the expression of ER chaperones that facilitate the correct folding or assembly of ER proteins and prevent their aggregation, thereby improving cell survival (3, 4, 6). However, when ER stress overwhelms the capacity of this intrinsic quality control, apoptosis is induced by up-regulation of the C/EBP homologous protein (CHOP).

In inherited diseases associated with ER stress, different mutations in the causative genes result in various phenotypes. One representative example, Pelizaeus-Merzbacher disease (PMD), is an X-linked recessive leukodystrophy characterized by diffuse hypomyelination in the central nervous system (CNS) (7). Missense mutations in the proteolipid protein 1 (*PLP1*) gene cause a wide spectrum of clinical phenotypes from a mild allelic disease, spastic paraplegia type 2 (SPG2) to severe connatal PMD (7). In these diseases, mutant proteins are misfolded and accumulate in the ER, leading to induction of ER stress and apoptosis of oligodendrocytes in the CNS (8, 9). However, little is known about how different mutations in the same gene induce ER stress differently and affect clinical severity. Factors, such as retention of misfolded proteins or the extent of UPR activation, may influence phenotypic variation (9–11). However, can any other factors contribute to the pathology of such ER stress-related disease? Here we focused on ER chaperones as a potential player. ER chaperones are highly conserved proteins that assist in protein folding. Therefore, it is generally believed that accumulation of misfolded proteins in the ER up-regulates chaperones to alleviate ER stress. In terms of its association with disease pathology, interaction between the mutant PLP1 and a major ER chaperone, calnexin (CANX), was shown to inhibit degradation of the misfolded mutant proteins (12). In the mutant superoxide dismutase model of amyotrophic lateral sclerosis (ALS), an ER stress-associated neurodegenerative disease, down-regulation of another chaperone, calreticulin (CALR), was shown to induce ER stress and trigger the death of mutant superoxide dismutase motoneurons (13). A recent study reported up-regulation of protein-disulfide isomerase (PDI, also referred to as P4HB), which is a chaperone in the ER catalyzing the formation and breakage of protein disulfides bonds, in microglia of transgenic mutant superoxide dismutase 1 mice (14). Therefore, we sought to determine whether changes in the expression of ER chaperones alter the accumulation of misfolded protein and ER stress, potentially modifying the cellular and clinical phenotypes.

For this purpose, we used PMD as a model and investigated missense *PLP1* mutations (8, 11). PLP1 with an A243V substitution (PLP1msd) is representative of the severe hypomyelination in myelin synthesis deficit (*msd*) mice (15) and humans (16), whereas two other mutations, W163L and I187T, are representative of the milder condition found in mild PMD/SPG2 patients (17, 18): the latter is also the mutation found in an SPG2 mouse model, *rumpshaker* (19). We also employed mutants in two other genes responsible for peripheral myelin disorders, a myelin protein zero (MPZ) mutant associated with a severe neuropathy, Dejerine-Sottas neuropathy (20), and two peripheral myelin protein 22 (PMP22) mutants that are associated with a clinically mild neuropathy, Charcot-Marie-Tooth disease (21–23).

In this study, we examined the expression of ER chaperones in response to mutants of *PLP1* and two other genes. Unexpectedly, we found that some ER chaperones were depleted rather than up-regulated. In addition, these mutant proteins induced fragmentation of the Golgi apparatus (GA). We also found an association between these changes and phenotypic severity. Furthermore, we proposed potential mechanisms underlying these cellular phenotypes. The results of this study suggest that changes in these subcellular organelles may contribute to the cellular pathogenesis and phenotypic severity of inherited ER stress-related diseases caused by mutant proteins.

EXPERIMENTAL PROCEDURES

Mice—Msd mice, which carry the spontaneous A243V mutation in the *Plp1* gene (15), were maintained in a B6C3F1/J background in accordance with the institutional guidelines of the National Center of Neurology and Psychiatry.

Plasmid Construction—Expression vectors for PLP1wt and PLP1msd were reported previously (24). *PLP1-W163L* and *PLP1-I187T* genes were generated by site-directed mutagenesis with modifications (25), and subcloned into pCAGGS (24), as fusions with N-terminal FLAG epitopes. Human wild-type and mutant *PMP22* and *MPZ* genes were amplified from cloned cDNAs (kind gift from Dr. JR Lupski) using appropriate primers and inserted into pCAGGS. For construction of an expression vector for the membrane-linked cell surface green fluorescent protein (GFP) as illustrated in Fig. 9*E*. The *GFP* gene was inserted into pDisplay (Invitrogen) in an in-frame manner. The *cytoplasmic luciferase* (*Cluc*) and *immunoglobulin (Ig) κ light chain* (*Igκ-Rluc*) genes were amplified from cloned cDNA (Promega) with appropriate primers, and cloned into pCDNA3.1 (Invitrogen) and pAP-Tag5 (GenHunter) to construct pCMV-Cluc and pCMV-Igκ-Rluc, respectively. To determine subcellular localization, the *Rluc* gene was inserted in-frame between the Igκ and myc sequences of pAP-Tag5 to make pCMV-Igκ-Rluc-Myc. The mouse myelin oligodendrocyte glycoprotein (*MOG*) gene was also amplified with appropriate primers using cDNA from postnatal day (P) 14-mouse spinal cord (SC), and cloned into pEGFP-N1 (Takara).

Chemicals and Antibodies—The following reagents were purchased from the suppliers indicated: brefeldin A (Wako), tunicamycin (Merck), thapsigargin (Sigma), lactacystin (Wako), and MG132 (Wako). The primary antibodies included mouse anti-PDI (Thermo Scientific, MA3-019), rabbit anti-CALR (Sigma, C4606), rabbit anti-GRP78 (Abcome, ab21685), rabbit anti-CANX (Enzo Life Sciences, ADI-SPA-860), mouse anti-CHOP (Santa Cruz Biotechnology, sc-7351), rabbit anti-GM130 (Abcome, ab52649), mouse anti-FLAG M2 (Sigma, F3165), rabbit anti-FLAG M2 (Cell Signaling, number 2368), mouse anti-c-Myc (Nacalai Tesque, MC045), rabbit anti-PLP (a kind gift from Dr. M. Itoh, NCNP), rabbit anti-Oligo2 (IBL 18953), mouse anti-myelin basic protein (MBP) (Covance, SMI-99P), mouse anti-action (Millipore, MAB1501), rabbit

anti-KDEL receptor (Santa Cruz Biotechnology, sc-33806) and mouse anti-ubiquitin (Santa Cruz Biotechnology, sc-8017) antibodies. Alexa Fluor-488, -594, and -647 secondary antibodies were purchased from Invitrogen. Horseradish peroxidase-labeled anti-mouse and rabbit antibodies were purchased from GE Healthcare.

Cell Culture—HeLa cells and human oligodendrocytic cells (MO3.13) were maintained in Dulbecco's modified Eagle's medium (DMEM, Thermo Scientific) supplemented with 20 units ml^{-1} of penicillin, 20 $\mu g\ ml^{-1}$ of streptomycin, and 10% fetal bovine serum. For transfection, HeLa cells were plated onto 6-well plates or 18-mm round coverslips in 12-well plates, and transfected with the indicated constructs using Lipofectamine 2000 (Invitrogen) or TransIt LT1 (Mirus), respectively, according to the manufacturers' protocols. After 24 h, transfected cells in the 6-well plates or on coverslips were subjected to immunoblotting, quantitative PCR and immunocytochemistry, respectively.

Mixed Glial Culture (MGC) Generated to Oligodendrocyte—MGCs were established from wild-type and *msd* mice, which were then differentiated into oligodendrocytes, as described by Abematsu *et al.* (26).

Immunoblot Analysis—HeLa cells and mouse SCs were lysed with TNE(+) lysis buffer (50 mM Tris-HCl, pH 8.0, 150 mM NaCl, 2 mM EDTA, 1% Triton-X-100, and 0.1% SDS) supplemented with protease and phosphatase inhibitors on ice for 10 min. For the digitonin fractionation experiment, HeLa cells were permeabilized with phosphate-buffered saline (PBS) containing 0.01% digitonin with protease and phosphatase inhibitors on ice for 10 min. After soluble proteins were collected, insoluble proteins were further treated with the TNE(+) lysis buffer. These extracts were centrifuged at 12,000 × *g* for 10 min to remove cell debris. Co-immunoprecipitation and cell surface biotinylation were performed as described previously (27). The cell extracts, co-immunoprecipitation and biotinylated samples, were subjected to immunoblotting with primary antibodies and horseradish peroxidase-labeled secondary antibodies. All immunoblot analyses were repeated at least 3 times with similar results. The relative protein expression levels on immunoblotting were quantified by an image analyzer.

Immunocytochemistry—HeLa cells, MO3.13 cells, and primary oligodendrocytes were fixed with 4% paraformaldehyde in PBS for 10 min, permeabilized with 0.1% Triton X-100 for 10 min, and treated with 3% bovine serum albumin to block nonspecific reaction. Detection of cell surface proteins, cells were not permeabilized by 0.1% TritonX-100. Cells were further incubated with the primary antibodies for 60 min at RT followed by visualization using the appropriate secondary antibodies labeled with Alexa-488, -594, or -647 with 4′,6-diamidino-2-phenylindole (DAPI). Apoptotic cells were detected using ApopTag kit (Chemicon), according to the manufacturer's protocol. These stained cells were observed with a confocal fluorescence microscope (FV-1000; Olympus).

Quantitative Reverse Transcriptase-Polymerase Chain Reaction—Total RNA was extracted from HeLa cells and mouse SCs and was converted to cDNA using SuperScript III reverse transcriptase (Invitrogen). Transcript levels were analyzed by a thermal cycler (7900HT; Applied Biosystems) with synthesized cDNA and the following pre-designed TaqMan probes (Applied Biosystems): human *GAPDH*, Hs99999905; human *CHOP*, Hs00358796; human *P4HB*, Hs00168586; human *CALR*, Hs00189032; human *GRP78*, Hs99999174; human *CANX*, Hs00233492; mouse *Gapdh*, Mm99999915; mouse *Chop*, Mm00492097; mouse *P4hb*, Mm01243184; mouse *Calr*, Mm00482936; mouse *Grp78*, Mm00517691; and mouse *Canx*, Mm00500330. Relative transcript levels were calculated by the $\Delta\Delta C_T$ method according to the manufacturer's standard protocol.

Luciferase Reporter Assay—HeLa cells were co-transfected with the Cluc and Igκ-Rluc genes along with pCDNA3.1-PLP1wt-FLAG, pCDNA3.1-PLP1msd-FLAG, or the empty vector. Activities for firefly luciferase and Igκ-Rluc in the cell lysate and supernatant were measured using a dual-luciferase assay system (Promega) according to the manufacturer's instructions. Relative Cluc and Igκ-Rluc activities in the supernatant were determined as ratios to cytosolic luciferase activity.

Statistical Analysis—Student's *t* test and analysis of variance were used for statistical analyses.

RESULTS

PDI, CALR, and GRP78 Are Depleted in the ER of HeLa Cells Expressing PLP1msd—Typically, when cells are under ER stress, ER chaperones are up-regulated as a part of the UPR. ER chaperones improve cell survival by facilitating the correct folding or assembly of misfolded proteins and preventing their aggregation (28). In HeLa cells, FLAG-tagged PLP1msd (PLP1msd-FLAG), a PMD-causing severe mutant known to induce ER stress (8) but not FLAG-tagged wild-type PLP1 (PLP1wt-FLAG), effectively co-immunoprecipitated GRP78 (Fig. 1*A*) and up-regulated the *CHOP* gene (Fig. 1*B*), a well characterized ER stress marker gene, indicating that this transient transfection system is applicable for analyzing cellular pathogenesis of ER stress caused by exogenous mutant proteins. To further analyze the changes in ER chaperone expression induced by this mutant PLP1, transfected HeLa cells were immunostained with antibodies against the FLAG epitope, PDI, CALR, GRP78, and CANX. Unexpectedly, we found that PDI, CALR, and GRP78 were drastically depleted, whereas CANX expression was unchanged (Fig. 1*C*). These changes were also observed in the human oligodendrocytic cell line MO3.13 (Fig. 1*D*), the human glioma cell line U-138, and simian kidney cell line COS-7 cells (data not shown). Almost 65% of the cells transfected with PLP1msd-FLAG had faint PDI, CALR, and GRP78 staining. This proportion was significantly higher than in cells transfected with PLP1wt-FLAG (Fig. 1*E*), suggesting that this phenomenon is due to the mutant PLP1, not the overexpression of PLP1 itself.

Next, we determined if reduced chaperone expression is caused by apoptotic cell death due to overwhelming ER stress. Cells expressing PLP1msd that had faint PDI immunostaining had no positive signal in the terminal deoxynucleotidyl transferase dUTP nick-end labeling (TUNEL) assay (Fig. 1*F*). Furthermore, depletion of PDI occurred as early as 6 h after transfection (Fig. 1*G*). These results suggest that PLP1msd impairs the ER chaperones independent of apoptosis.

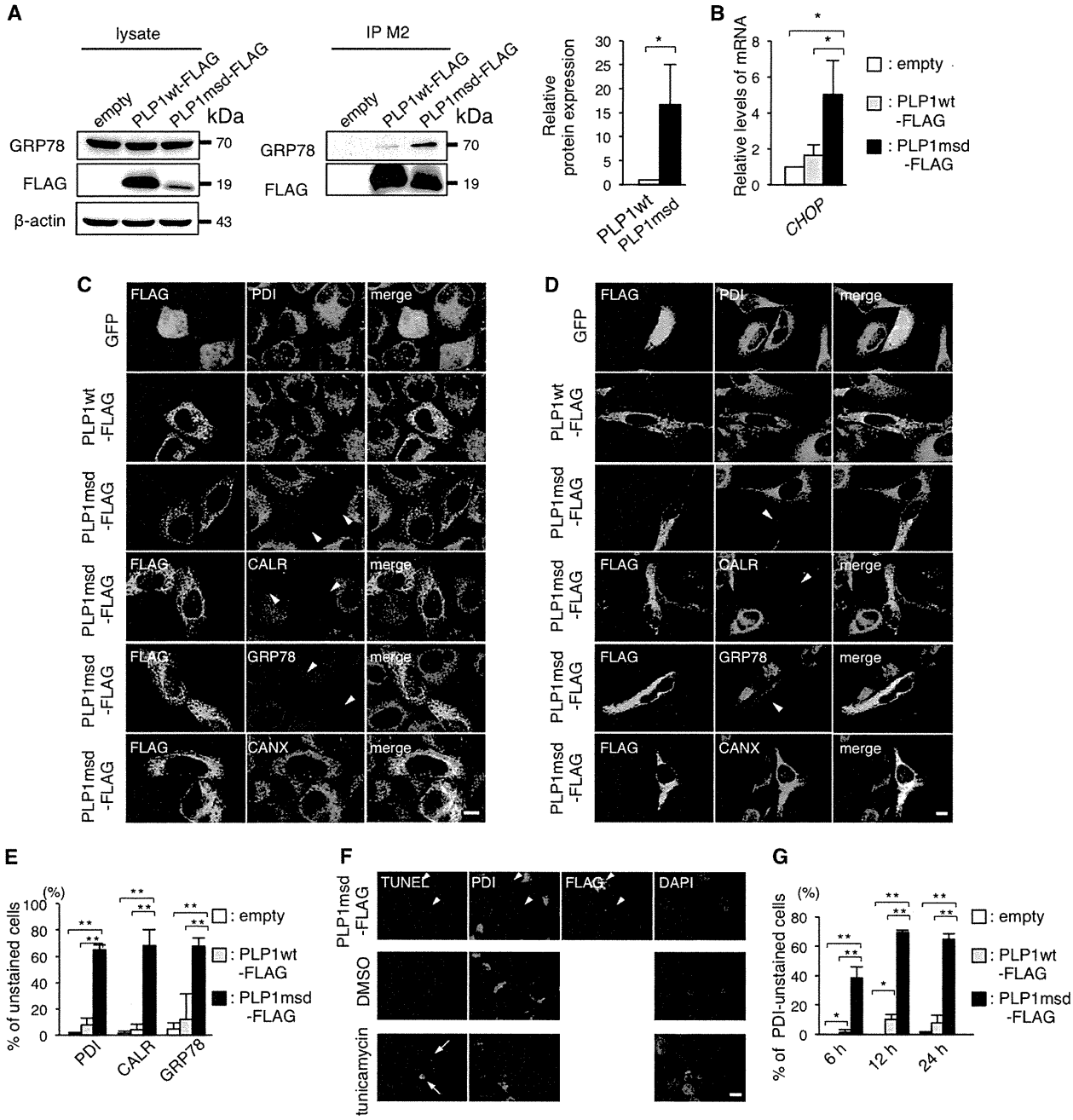

FIGURE 1. **PLP1msd overexpression resulted in a negative ER chaperone staining pattern.** *A*, co-immunoprecipitation of PLP1 with GRP78 in HeLa cells. *B*, quantitative RT-PCR for the *CHOP* gene in HeLa cells expressing PLP1wt or PLP1msd. The *GAPDH* gene was used as an internal control. Results are represented as fold-induction compared with empty vector-transfected control experiment. Values are represented as the mean ± S.E. from three independent experiments (*, $p \leq 0.05$). *C* and *D*, immunocytochemistry of ER chaperones in HeLa cells (*C*) and human oligodendrocytic cells, and MO3.13 cells (*D*) expressing PLP1wt or PLP1msd. Cells transfected with the indicated vectors were immunostained with an anti-FLAG antibody (*green*) together with anti-PDI, anti-CALR, anti-GRP78, or anti-CANX antibodies (*magenta*) and observed with a confocal fluorescence microscope. Note that cells expressing PLP1msd showed an extremely faint staining pattern (*arrowheads*) for PDI, CALR, and GRP78, but not for CANX. *Scale bar*, 10 μm. *E*, the proportion of unstained cells for PDI, CALR, and GRP78. *F*, apoptosis of HeLa cells expressing PLP1msd. TUNEL assay combined with immunocytochemical staining using the anti-FLAG (*white*) and anti-PDI (*magenta*) antibodies. Tunicamycin treatment served as a positive control for TUNEL (*arrow*). None of the PLP1msd-positive cells showed positive signals for TUNEL (*arrowheads*). *Scale bar*, 10 μm. *G*, time course of the proportion of PDI negative HeLa cells transfected with the PLP1msd gene. The results are represented as the mean ± S.E. from three independent experiments with >100 cells counted in each experiment (*, $p \leq 0.05$; **, $p \leq 0.005$).

Expression of PLP1msd Translocates the ER Chaperones from the ER—To examine whether PLP1msd depletes the chaperones by inhibiting their transcription in HeLa cells, we performed quantitative real time-polymerase chain reaction (RT-PCR) (Fig. 2*A*). As we demonstrated previously (24), *GRP78* mRNA expression was increased significantly in cells transfected with PLP1msd-FLAG compared with cells transfected with PLP1wt-FLAG. The expression of *PDI* and *CALR* was slight, but significantly up-regulated. These results indicate that PDI, CALR, and GRP78 are depleted in the ER without

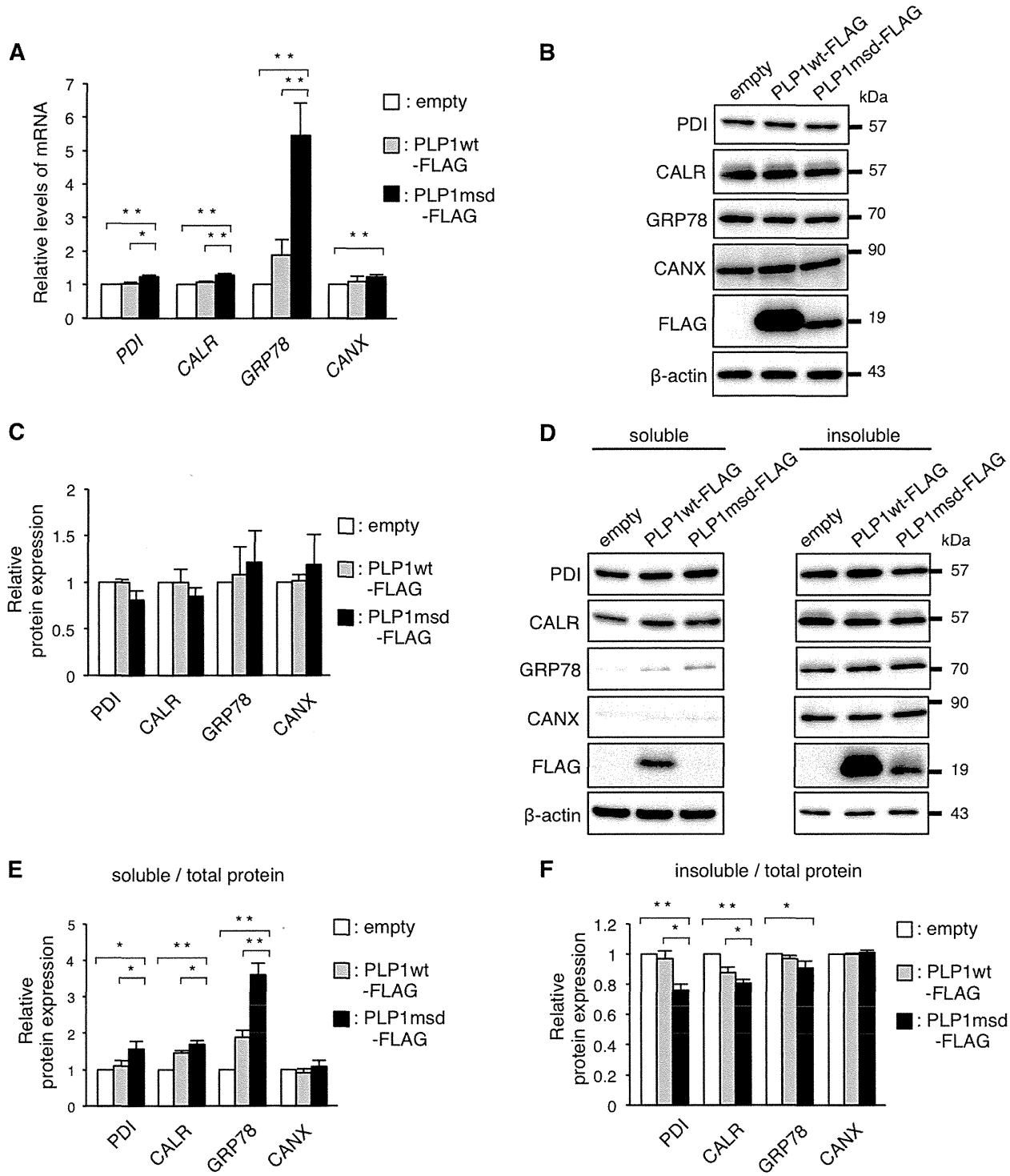

FIGURE 2. **PDI, CALR, and GRP78 are depleted from the ER without decreasing their transcripts.** *A*, relative expression of the transcripts of the ER chaperones in HeLa cells transfected with the PLP1 genes. Expression levels of *PDI*, *CALR*, *GRP78*, and *CANX* mRNA were analyzed by quantitative RT-PCR and normalized to *GAPDH*. The results are represented as fold-induction against the control experiment (empty vector transfection). *B* and *C*, total amount of the ER chaperones in HeLa cells transfected with PLP1wt-FLAG and PLP1msd-FLAG. Protein samples from the cells transfected with the indicated vectors were subjected to immunoblotting with the indicated antibodies (*B*). The amounts of the proteins were measured by densitometry and normalized to β-actin. The results are represented as fold-induction against the control experiment using the empty vector (*C*). *D–F*, subcellular fractionation analysis using 0.01% digitonin. Transfected cells were treated with 0.01% digitonin followed by 0.1% SDS, 1% Triton X-100. The extracts of digitonin soluble (*left*) and insoluble fraction (*right*) were subjected to immunoblotting with the indicated antibodies (*D*). The blots were quantitatively analyzed by densitometry to measure the proportion of soluble fraction (*E*) and insoluble fraction (*F*) in each protein. Bar graphs are represented as fold-induction ± S.E. against the mean of control experiment from three independent experiments (*, $p \leq 0.05$; **, $p \leq 0.005$).